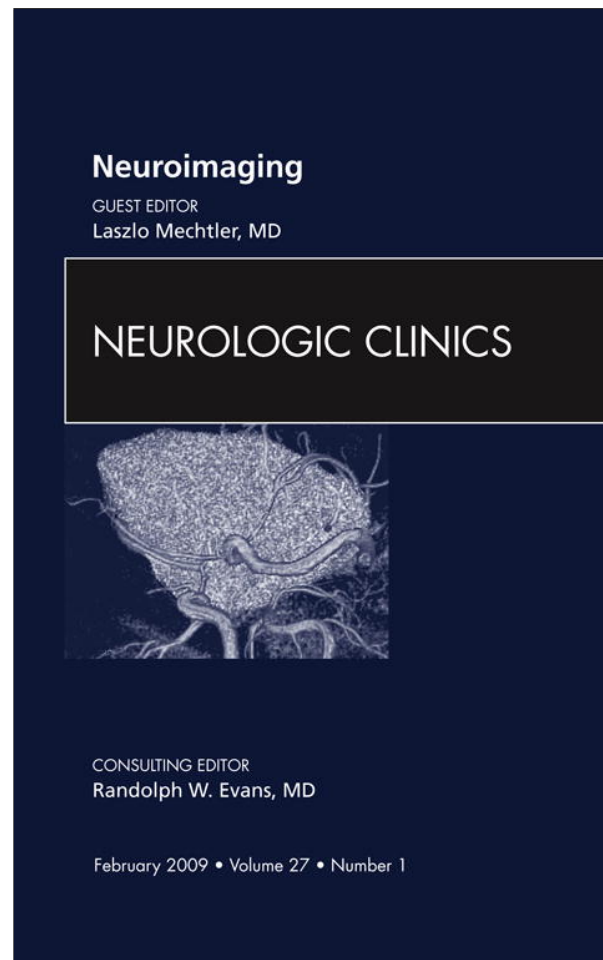


Provided for non-commercial research and education use.
Not for reproduction, distribution or commercial use.



This article appeared in a journal published by Elsevier. The attached copy is furnished to the author for internal non-commercial research and education use, including for instruction at the authors institution and sharing with colleagues.

Other uses, including reproduction and distribution, or selling or licensing copies, or posting to personal, institutional or third party websites are prohibited.

In most cases authors are permitted to post their version of the article (e.g. in Word or Tex form) to their personal website or institutional repository. Authors requiring further information regarding Elsevier's archiving and manuscript policies are encouraged to visit:

<http://www.elsevier.com/copyright>

Neuroimaging in Neuro-Oncology

Laszlo Mechtler, MD

KEYWORDS

• Brain tumors • MRI • Neuroimaging • Neuro-oncology

The introduction of MRI into clinical practice has been among the most important of all advances in the care of patients with brain tumors. Neuroimaging is no longer a tool simply to evaluate structural abnormalities and identify tumor-related complications but has evolved into a science that incorporates functional, hemodynamic, metabolic, cellular, and cytoarchitectural alterations. Where previously, pathologic and anatomic imaging has offered information about histologic diagnosis, past imaging has never incorporated information about the actual biologic behavior of these neoplasms. Today, a multitude of new imaging techniques exist that have revolutionized neuro-oncologic imaging. This article reviews neuroimaging with an emphasis on advanced MRI techniques in the field of neuro-oncology.

Brain and other intracranial central nervous system (CNS) tumors are a heterogeneous group of neoplasms. They vary widely by site of origin, morphologic features, genetic alterations, growth potential, extent of invasiveness, tendency for progression or recurrence, and treatment response. An estimated 51,410 new cases of primary benign and malignant brain tumors are diagnosed annually in the United States, including 3750 cases in children and adolescents. Approximately 16.5 per 100,000 person-years in the United States will be diagnosed with a primary nonmalignant and malignant brain and CNS tumors each year. Of this group, 7.3 per 100,000 person-years have malignant tumors.¹ Malignant brain tumors are the leading cause of death from solid tumors in children and the third-leading cause of cancer-related death in patients aged 15 to 34 years old.² Metastatic brain tumors are even more common and affect between 100,000 and 150,000 new patients each year in this country.³

Neuroimaging of brain and CNS tumors can be divided into four broad categories: (1) tumor diagnosis, (2) preoperative treatment planning, (3) intraoperative imaging, and (4) postoperative care and treatment response.

The current standard of neuroimaging for brain tumor evaluation is anatomic MRI with gadolinium-based intravenous contrast agent, providing highly sensitive tumor detection and characterization far superior to any other imaging modality. MRI has been found to be more sensitive than CT in the detection of asymptomatic progression

DENT Neurologic Institute, 3980 Sheridan Drive, Amherst, NY 14226, USA
E-mail address: lmechtler@dentinstitute.com

Neurol Clin 27 (2008) 171–201

doi:10.1016/j.ncl.2008.09.015

0733-8619/08/\$ – see front matter © 2008 Elsevier Inc. All rights reserved.

neurologic.theclinics.com

of disease. However, conventional MRI suffers from nonspecificity with respect to vastly different pathologic processes that appear to be similar on imaging. In the last decade, the development and application of various functional imaging techniques have increased, such as proton MR spectroscopy (pMRS) and diffusion/perfusion-weighted MRI (DWI/PWI). The implementation of many of these more advanced, time-consuming, functional methods has lagged behind that of the conventional MRI techniques. Several factors account for this observation, among which are the lack of physician–clinician education, the absence of standardization, and delays in reimbursement by Medicare and therefore by many private insurers.

The advantages of MRI are its multiplanar capability, superior contrast agent resolution, and flexible protocols that play an important role in assessing tumor location and extent, in directing biopsies, in planning proper therapy, and in evaluating therapeutic results. Preoperative imaging of a brain tumor plays several important roles, including characterization of the brain tumor, providing preliminary information of tumor type and grade, establishing a differential diagnosis, providing sufficient anatomic detail for surgical planning, and identifying tumor-related complications such as hemorrhage, hydrocephalus, herniation, or mass effect. Intraoperative imaging has improved neurosurgical morbidity and increased the amount of tumor resected, which is associated with improved quality of life and increased survival of patients. Postoperative imaging is important to monitor treatment response and detect tumor progression as early as possible. Imaging will often detect tumor progression before clinical deterioration occurs.

ROUTINE MR SEQUENCES IN NEURO-ONCOLOGY

Characterization of brain tumors by MRI involves determining, in the context of the patient's age and sex, the location of the lesion and whether and how it enhances after gadolinium injection. The fundamental question asked by the imager is whether the mass is intra-axial (intraparenchymal) or extra-axial (extraparenchymal). As a general rule, most brain tumors have prolonged T1 and T2 relaxation times and therefore appear hypointense relative to normal brain on T1-weighted images and hyperintense on T2-weighted images. The degree of enhancement is variable, depending on the vascularity of the lesion and the integrity of the blood–brain barrier of the intratumoral vessels. Increased enhancement is usually suggestive of a higher-grade tumor.

Fluid-Attenuated Inversion Recovery

Fluid-attenuated inversion recovery (FLAIR) imaging is a sequence that produces heavily T2-weighted images with cerebrospinal fluid (CSF) nulling by using an inversion pulse placed at the CSF null point, followed by long echo time readout. Fast-FLAIR images provide better definition between edema and tumor. Contrast-enhanced FLAIR MRI has been used successfully in taking advantage of the T1 effect to achieve particular high contrast between tumor and background tissue. Contrast FLAIR has also been used in the identification of leptomeningeal disease in patients who have metastases.^{4,5} FLAIR is not as sensitive in detecting posterior fossa abnormalities as is fast spin-echo T2-weighted imaging.^{6,7}

Short tau Inversion Recovery and Spectral Inversion Recovery

Short tau inversion recovery (STIR) uses an inversion prepulse to selectively suppress fat signal and improve long T1/long T2 lesion enhancement. This form of fat suppression is particularly useful for avoiding chemical shift artifacts.⁸ It is commonly used to differentiate lipomas from other lesions, such as hemorrhage. It is also used routinely

to evaluate tumors of the orbits and within the bone marrow, two structures that commonly contain an abundance of fat. Whole-body turbo STIR MRI is now used routinely in detecting skeletal metastases in diseases such as multiple myeloma.⁹ Lipid-specific fat saturation, such as spectral inversion recovery, is helpful for contrast-enhanced T1-weighted imaging in areas with a large amount of fat.

Gradient-Echo Imaging

In gradient-echo (GE) pulse sequences, the 180° refocusing pulse is omitted and a flip angle smaller than 90° is used, thereby significantly reducing scan time. Because susceptibility effects are not refocused, blood products and iron, calcium, and manganese deposition are seen more readily with GE sequences. In addition, GE imaging is sensitive to flow, and therefore has been the most common method for MR angiography. GE imaging is used to clarify focal linear regions of signal void within a mass, whether they represent dense calcification or flow within the tumor vessels. It is especially useful in finding hemosiderin in brain tumors that have a predilection to bleed, including metastases such as melanoma and renal cell carcinoma and primary brain tumors such as oligodendrogliomas, ependymomas, and glioblastoma multiforme (GBM). In patients who have received brain radiation, the use of GE is more sensitive than T2-weighted imaging for the detection of hemosiderin from radiation-induced occult vascular malformations.¹⁰ Echo-planar imaging uses rapid gradient switching instead of repeated radio-frequency excitations, resulting in much shorter scan times than conventional GE imaging. Single-shot echo-planar imaging is the fastest form of MR acquisition but may be limited in resolution or suffer from artifacts, depending on hardware configuration. Multishot echo-planar imaging can be used to mitigate these shortcomings and is generally superior to single-shot sequences in terms of lesion conspicuity and delineation.¹¹

Magnetization Transfer Imaging

Magnetization transfer imaging uses off-resonance prepulses to reduce signal from semisolid tissue, like brain parenchyma, relative to signal from more fluid components, such as blood. Magnetization transfer contrast improves lesion detection with gadolinium. In fact, 40% or more metastases were identified when magnetization transfer contrast was used with single-dose contrast administration, and even more lesions were detected with triple-dose contrast.^{12,13}

MR Venography, Angiography, and Cerebrospinal Fluid Flow Studies in Brain Tumors

It is useful to perform MR venography in patients who have tumors adjacent to venous channels, such as the superior sagittal sinus, to confirm its patency (**Fig. 1**), especially when dealing with convexity and falx meningiomas.¹⁴

MR angiography should be obtained when arteries perforate or are compromised by intracranial tumors, especially around the skull base. Although MR angiography and CT angiography are excellent tests for arterial compromise or distortion, conventional angiography is still the gold standard. Cine CSF flow studies using cardiac-gated dynamic GE MRI are indicated whenever it is necessary to evaluate the flow of CSF and to rule out an obstruction within the CSF pathways due to brain tumors. In addition to a qualitative visualization, a dynamic phase-contrast acquisition may be useful to provide a quantitative map of CSF flow patterns.

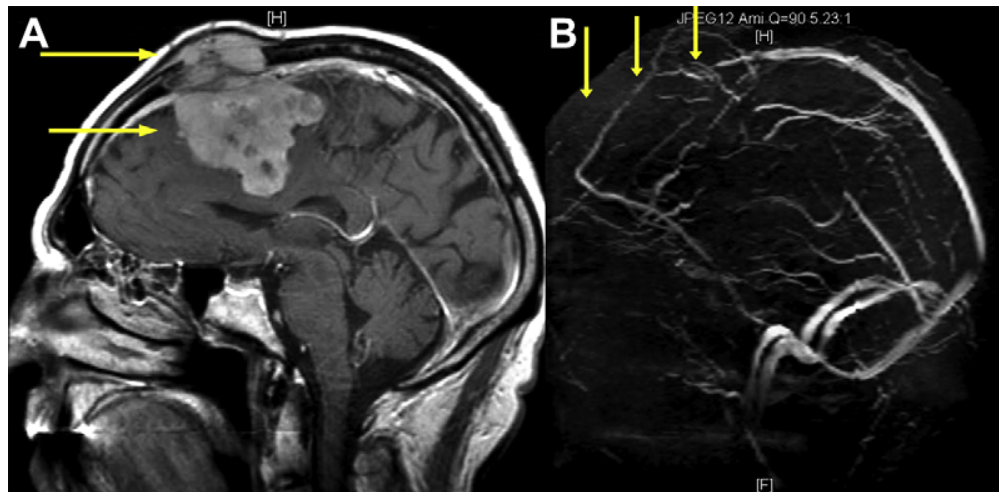


Fig. 1. A 70-year-old man presents with a bump on the head and headaches. A preoperative T1-weighted contrast study (A) shows an enhancing frontal lobe mass (*horizontal arrows*) extending through the calvarium and raises the scalp. MR venography (B) confirms an occlusion of the superior sagittal sinus (*vertical arrows*). The use of MR venography is essential for the appropriate work-up of falx meningiomas adjacent to the superior sagittal sinus.

Short T1 and T2 in Neuro-oncology

During the evaluation of tumors, it is helpful to recognize MR signal characteristics not typically seen in brain tumors. In general, brain tumors are hypointense on T1-weighted images and hyperintense on T2-weighted images, reflecting increased water content of the neoplasm and vasogenic edema. This “long T1 and long T2” is the most common signal intensity in brain tumors, but knowledge of the exceptions to this rule is vital in establishing a more precise differential diagnosis. Exceptions include tumors that have T2-weighted hypointensity (short T2), which includes neoplasms that have paramagnetic effects, due to iron, hemosiderin, deoxyhemoglobin, and melanin. In addition, hypointensities on T2 include calcification, high nucleus-to-cytoplasm ratio (ie, primitive neuroectodermal tumor, lymphoma), dense cellularity, fibrocollagenous stroma, high protein concentration, and signal flow voids from rapid flow. It is important to recognize hyperintensities (short T1) on noncontrast T1-weighted images, including methemoglobin, melanin, some forms of calcification, natural-occurring ions associated with necrosis (such as manganese, iron, and copper), high protein, fat, and flow-related enhancement in tumor vessels. These areas of short T1, short T2 will allow the interpreter a differential diagnosis that is far more specific.¹⁵

Box 1 summarizes findings of short T1 and short T2 in brain tumors.

Gadolinium

The routine use of contrast MR for the monitoring of brain tumors is the standard of care in neuro-oncology. In the surveillance of malignant gliomas, it is justifiable to obtain imaging every 2 months. In patients who have astrocytomas or oligodendrogliomas, MRI every 4 to 6 months is more the routine.¹⁶ Postoperatively, gadolinium-enhanced MRI should be performed within 72 hours, preferably the next day, to minimize the enhancement surrounding the postoperative cavity.¹⁷ The accepted standard dose for gadolinium is 0.1 mmol/kg. In an attempt to improve delineation of the extent of primary brain tumors and sensitivity for brain metastases, higher doses of gadolinium have been used, including 0.3 mmol/kg. Recently, the use of gadolinium has been associated with nephrogenic systemic fibrosis (NSF) in patients who have kidney failure. Gadolinium is normally excreted through the urinary system within

Box 1**Short T1 and T2 in neuro-oncology***Short T1 (hyperintensity)*

Methemoglobin (subacute blood)
 Melanin (melanoma)
 Manganese
 Iron
 Copper
 High protein (colloid cyst, craniopharyngioma)
 Fat (lipoma, dermoid)
 Cholesterol
 Paramagnetic agent (gadolinium)
 Flow-related enhancement in tumor vessel
 Calcium

Short T2 (hypointensity)

Iron within necrosis (GBM)
 Hemosiderin (chronic bleed)
 Deoxyhemoglobin (acute bleed)
 Melanin (melanoma)
 Ferritin
 Calcification (oligodendroglioma)
 High nucleus/cytoplasm ratio (primitive neuroectodermal tumor, lymphoma)
 Dense cellularity
 Macromolecule content
 Fibrocollagenous stroma (meningioma)
 Mucin (colon carcinoma)
 High protein content (craniopharyngioma)
 Fast-flowing blood (hemangioblastoma, GBM)

6 hours post infusion, but elimination becomes problematic for individuals who have reduced kidney function. The half-life is prolonged and may increase to 30 to 120 hours in this patient population.¹⁸

The most important factors associated with the development of NSF are dialysis and moderate or end-stage renal disease (glomerular filtration rate less than 30 mL/minute/1.7 m²). NSF is also evident with repeated or high doses of gadolinium normally seen with extracranial MR angiography. NSF is a debilitating and sometimes fatal disease affecting the skin, muscle, and internal organs. Although gadolinium is ordered routinely in the evaluation of intra- and extra-axial brain tumors, caution must be exercised in any patient who has renal failure or is receiving dialysis.^{19,20}

IMAGING CHARACTERISTICS OF BRAIN TUMORS

The characterization of brain tumors on MRI involves an initial determination as to whether the mass is actually a neoplasm. The goal is to provide a brief and relevant

differential diagnosis. Despite improvements in technology, one has to be cognizant that neuroimaging does not equate with tissue diagnosis; therefore, caution must always be used when interpreting imaging findings. Tumors of neuroepithelial origin are made up of a large and diverse group of neoplasms, with a mixture of slow-growing and malignant tumor types. Gliomas, in particular, can grow diffusely within the brain or can be more circumscribed. The more circumscribed tumors are pilocytic astrocytoma, pleomorphic xanthoastrocytoma, and subependymal giant cell astrocytoma. Pilocytic astrocytoma and subependymal giant cell astrocytoma are World Health Organization (WHO) grade I neoplasms. By far, the most common gliomas are astrocytoma (WHO grade II), anaplastic astrocytomas (WHO grade III), and GBM (WHO grade IV).²¹

Circumscribed Astrocytomas

In general, the presence of contrast enhancement correlates with increasing grade of tumor. Exceptions to this rule of enhancement within the family of gliomas include pilocytic astrocytomas, pleomorphic xanthoastrocytoma, and subependymal giant cell astrocytomas.

Pilocytic astrocytomas represent 2% to 6% of all primary brain tumors. They often arise from the midline structures, such as the optic nerve, hypothalamus, brainstem, and cerebellum. On MRI, they represent well-circumscribed tumors with benign morphologic features.²² Pilocytic astrocytomas have a more benign clinical course, especially when they occur in patients who have neurofibromatosis type 1. They display contrast enhancement in 94% of cases, which is related to the vascular nature of these tumors. Two thirds of all cases demonstrate the classic imaging manifestation of a cyst-like mass with an enhancing mural nodule. Although most cyst walls do not enhance, some may enhance intensely, even as much as the mural nodule.^{23,24}

Pleomorphic xanthoastrocytomas are generally WHO classification grade II and cases of malignant transformation are rare. These lesions usually occur in adolescents or young adults (average age of 26 years), although a wide age range is reported (5–82 years). Pleomorphic xanthoastrocytoma presents as either a cyst with a mural nodule or a solid tumor. The mural nodule is usually attached to the leptomeninges. Involvement of the leptomeninges is highly characteristic, seen in 71% of cases in one series.^{25,26} MRI usually reveals a mass that has similar signal intensities on T1-weighted images to the gray matter and increased signal intensities on T2-weighted images. In addition, imaging features of these lesions typically show a lack of significant peritumoral edema and a scalloping of the adjacent calvaria. Furthermore, with contrast injection, intense enhancement of the mural nodule of the solid tumor is seen. The wall of the cyst may or may not be enhanced.

Subependymal giant cell astrocytomas typically occur adjacent to the lateral ventricle and are seen in 6% to 16% of patients who have tuberous sclerosis. On MRI, these tumors show mixed signal intensities in T1- and T2-weighted images, and homogeneous contrast enhancement is typical. They have a typical location adjacent to the foramen of Monro and are commonly associated with other features of tuberous sclerosis, including cortical tubers and subependymal nodules.^{27,28} **Fig. 2** provides examples of circumscribed astrocytomas.

Astrocytomas

Diffuse astrocytomas are uncommon before the age of 10 and after the age of 65. The mean age of presentation is 34 years with a slight male predilection, and they represent 25% to 30% of gliomas in adults. The most frequently encountered subtypes are fibrillary, protoplasmic, and gemistocytic, with the last more often associated

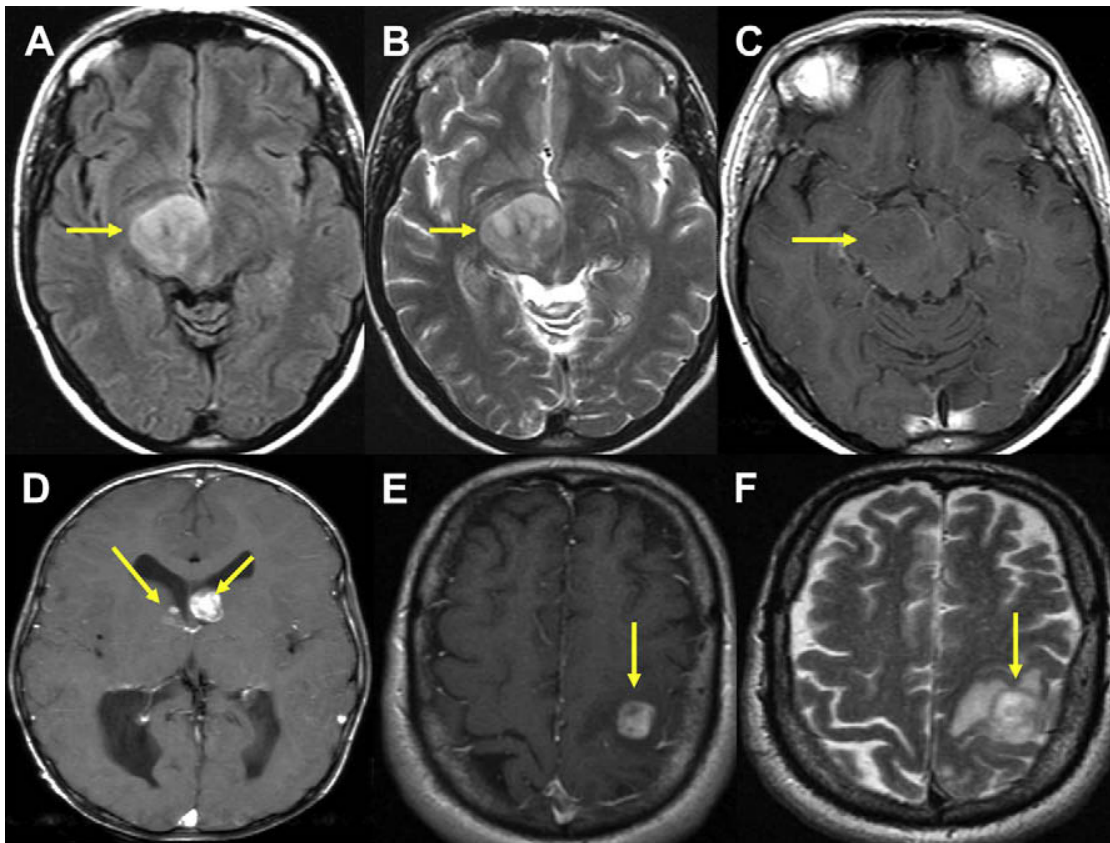


Fig. 2. Circumscribed astrocytomas. FLAIR (A), T2-weighted image (B), and T1-weighted image (C) show a well-circumscribed right midbrain ovoid mass in a 23-year-old woman presenting with numbness in the left hand. This solid tumor is hyperintense on FLAIR and T2-weighted images and iso-hypointense, but nonenhancing on T1-weighted contrast images. Stereotactic biopsy confirms a pilocytic astrocytoma. The patient continues to be doing well 10 years after diagnosis. T1-weighted contrast image (D) shows bilateral enhancing masses adjacent to the foramen of Monro in a patient who has tuberous sclerosis complex. The diagnosis is subependymal giant cell astrocytoma. Axial T1-weighted contrast (E) and T2-weighted (F) images show a round enhancing left posterior frontal lobe mass associated with mild vasogenic edema. Pathology was consistent with a pleomorphic xanthoastrocytoma.

with malignant transformation.²⁹ Histologically, these tumors consist of normal-appearing astrocytes, but with hypercellularity. Mitosis, hemorrhage, and necrosis are notably absent. Astrocytomas often appear homogeneous and infiltrating. They display a low signal on T1-weighted images and a high signal on T2-weighted images, with little to no contrast enhancement. The absence of contrast enhancement is consistent with the absence of any vascular changes histologically. Any enhancement in an astrocytoma suggests progression to a higher grade.³⁰ Among cases of astrocytoma, approximately two thirds are supratentorial in location, predominantly involving the subcortical white matter. FLAIR imaging is probably the most sensitive sequence for the detection of these slowly infiltrating neoplasms,³¹ whereas CT imaging reveals tumoral calcification in 20% of cases. In this setting, GE MR images may also help in evaluating for calcification.

Anaplastic Astrocytomas

WHO grade III AA is an infiltrating tumor with biology intermediate between astrocytoma and GBM. It occurs most commonly between 40 and 50 years of age.³² Although some AAs arise as new primary “de novo” tumors, 75% result from dedifferentiation of

an astrocytoma. AA is characterized by hypercellularity, mitotic activity, and nuclear atypia without necrosis. Scattered areas of nodular gadolinium enhancement show the presence of newly formed blood vessels that have an abnormal blood–brain barrier. These tumors may show moderate expansion of the involved brain regions and may also show evidence of significant surrounding vasogenic edema. Gadolinium ring enhancement of such a tumor, however, would likely represent a GBM, and not an AA.³³

Gliomatosis cerebri is a rare brain neoplasm that is characterized by a diffuse infiltration of malignant glial cells throughout large regions of the CNS. In the WHO classification of brain tumors, gliomatosis cerebri is described as a diffuse glial tumor extensively infiltrating the brain, involving more than two lobes (frequently bilaterally), and often extending to infratentorial structures. Islands of anaplasia are often found that may enhance with contrast and 19% may extend into the cortex.^{34,35} The best diagnostic clue for gliomatosis cerebri is a T2 hyperintense infiltrating mass with enlargement of involved structures and predominant subcortical location affecting more than one lobe, with subtle areas of enhancement.

Glioblastoma Multiforme

Accounting for more than one half of all gliomas and 15% to 20% of intracranial tumors, GBM is the most common malignant primary brain tumor. It may occur at any age but most commonly affects adults, with a peak incidence between 45 and 70 years of age. GBMs usually occur within the subcortical white matter, where they may present de novo as a primary GBM or after dedifferentiation from lower-grade glioma (secondary). It is felt that 60% of these tumors are de novo in adults older than the age of 50 years. Secondary GBM typically develops in younger patients under the age of 45 years through malignant progression from a low-grade astrocytoma or AA. GBM is often associated with pronounced mass effect and vasogenic edema due to a breakdown in the blood–brain barrier. Heterogeneous enhancement with centrally nonenhancing regions is consistent with necrosis.³⁶ Imaging may show distinct changes that are not consistent with the pathologic report. An example of this is a diffuse astrocytoma by biopsy that may have enhancement, or even evidence of necrosis, on imaging. Despite the pathology report, these tumors should be monitored by MRI with the same frequency as with a high-grade tumor. The possibility of a high-grade histopathology in a nonenhancing astrocytoma rises substantially with age, such that by 45 years of age, the chance is approximately 50%. These facts imply not only that all nonenhancing masses suspected to represent gliomas should be biopsied but also that the intrinsic heterogeneity of gliomas means that imaging tools are needed to help neurosurgeons choose the part of the tumor for biopsy that probably contains the high-grade tumor, if present.³¹

The imaging and pathologic hallmark of GBM is necrosis.³⁷ Besides necrosis, hemorrhage can occur in up to 19% of patients who have GBM. On T2-weighted images, GBM appears to be a heterogeneous mass with high signal intensity. The heterogeneous appearance may be due to central necrosis, hemorrhage, and tumor vascularity. Vasogenic edema, which surrounds the tumor, extends along the adjacent white matter tracts and usually produces significant mass effect. The vasogenic edema is produced by abnormal neoplastic vessels that lack the normal blood–brain barrier, resulting in transudation of fluids and proteins into the extracellular space. GBMs disseminate most commonly along the white matter tracts to involve the contralateral hemisphere, especially across the corpus callosum. Symmetric extension through the corpus callosum gives rise to a butterfly appearance. Most GBMs are solitary lesions. Multifocal and multicentric tumors occur in about 10% and 1% of cases,

respectively. Multicentric tumors are described as widespread lesions in different lobes of the hemispheres without evidence of intracranial spread or microscopic connection.³⁸ On the other hand, those with either gross or microscopic continuity are defined as multifocal.

Patients who present with de novo GBM commonly have symptoms after a short period of time and have no known history of previous low-grade astrocytoma. These patients typically are older adults, with tumors that overexpress epidermal growth factor receptor and rarely have alterations in tumor protein p53. Conversely, patients who have GBM arising from a known, low-grade astrocytoma tend to be younger, and many of these tumors have chromosome p53 mutation and a loss of heterozygosity of chromosome 17p but rarely overexpress epidermal growth factor receptor.³⁹

One of the major frustrations in the field of neuro-oncology is the difficulty in determining the biologic behavior of brain tumors on the basis of tissue diagnosis and imaging studies. It is not uncommon to see a low-grade, diffuse, fibrillary astrocytoma change in behavior and become more aggressive within a period of months after the initial diagnosis. This development is called anaplastic progression or dedifferentiation and results from a stepwise accumulation of molecular genetic changes within tumor cells. Although precise numbers are difficult to determine, approximately 50% of low-grade diffuse fibrillary astrocytomas undergo radiographically detectable anaplastic progression, with the remainder showing gradual growth as a low-grade lesion.⁴⁰

Oligodendrogliomas

Oligodendrogliomas are glial tumors that arise from oligodendrocytes. They account for approximately 5% to 10% of all intracranial neoplasms, most commonly affecting the frontal lobes. Most patients present at 35 to 40 years of age. Marked enhancement tends to be associated with anaplastic grades.⁴¹ Calcifications may be more conspicuous on GE sequences. Loss of chromosomes 1p and 19q is associated with an indistinct border on T1-weighted images and mixed intensity signal on T1-weighted and T2-weighted sequences, in conjunction with paramagnetic susceptibility effect due to calcification (a common histopathologic finding in oligodendrogliomas).⁴²

Astrocytomas and oligodendrogliomas cannot be differentiated from one another on the basis of imaging alone, although some characteristics favor oligodendrogliomas, such as cortical involvement, presence of calcification, and heterogeneous signal, including, in some cases, the presence of an intratumoral cyst and subtle patchy enhancement.⁴³ Clinically speaking, the involvement of the cortex can explain why patients who have oligodendrogliomas often present with seizures (**Fig. 3**). In addition, this tumor has a higher tendency to hemorrhage and, for this reason, the paramagnetic effects of blood products and calcification are best delineated by GE imaging.

In astrocytoma or oligodendroglioma imaging, every new MRI study should be compared with previous studies over as long a period of time as possible to detect the presence of gradual interval growth. Oligodendrogliomas have been found to grow approximately 4 mm in cross-section diameter over a period of 1 year.⁴⁴ The gradual growth of these low-grade infiltrative tumors indicates that therapeutic intervention should be considered. In cases where the patient is receiving treatment, tumor growth is a sign of resistance to therapy. Anaplastic progression is seen more commonly with increased mass effect, increasing vasogenic edema, and new foci of enhancement.⁴⁵

Ependymomas

Ependymomas are glial tumors derived from differentiated ependymal cells lining the ventricles of the brain and the central canal of the spinal cord. Ependymomas are

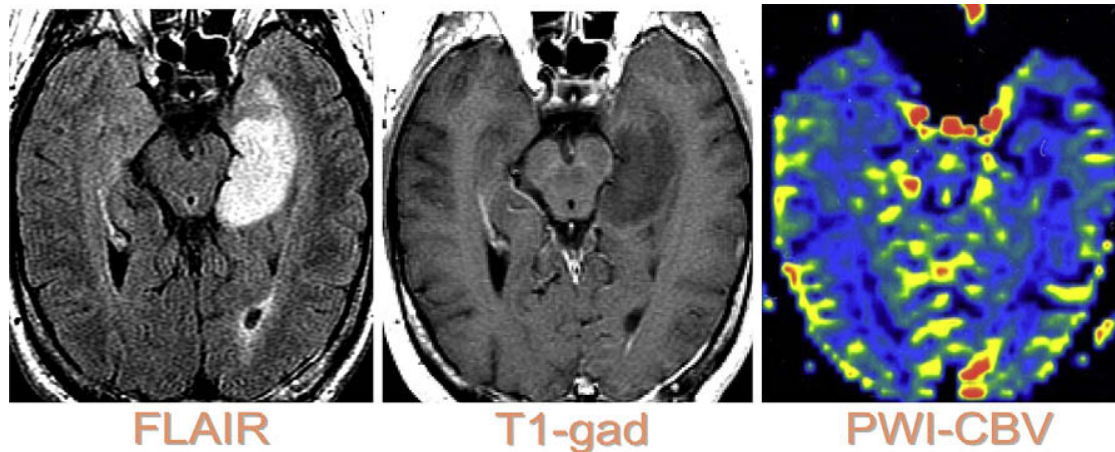


Fig. 3. A 24-year-old woman who presented with a complex partial seizure. The FLAIR image shows a hyperintensity involving the left mesial temporal lobe with cortical and subcortical involvement. T1-weighted hypointensity shows no enhancement and PWI lacks any evidence of increased perfusion consistent with oligodendroglioma WHO II. After complete resection, no further treatment was recommended. CBV, cerebral blood volume.

common tumors in children, accounting for about 10% of pediatric CNS neoplasms and about 5% of all gliomas. CSF dissemination occurs in up to 17% of patients. Forty percent of ependymomas are supratentorial, whereas 60% are infratentorial in location. Because of its intraventricular location, infratentorial ependymoma will become clinically symptomatic earlier, secondary to increased intracranial pressure and obstructive hydrocephalus. Supratentorial ependymomas are more often malignant than infratentorial ependymomas (malignant in 85% of supratentorial versus 50% of infratentorial cases).⁴⁶ On T1-weighted images, these lesions are usually iso-hypointense and will commonly squeeze through the fourth ventricular foramina into the cisterns. Generally, posterior fossa ependymomas have an indistinct interface with the floor of the fourth ventricle. On CT imaging, calcium is a common (50%) finding and typically is punctate. On T2* GE images, “blooming,” or hypointensity of calcium or hemosiderin, is often seen. Posterior fossa cysts occur uncommonly (15%) and are small, whereas supratentorially, they are more often seen associated with large cysts (80%). Variable mild-to-moderate heterogeneous enhancement is seen.⁴⁷

Primary Central Nervous System Lymphoma

Primary CNS lymphomas (PCNSL) are high-grade non-Hodgkin’s B-cell lymphomas in 98% of cases. The incidence is increasing in immunocompetent and immunocompromised individuals. Immunocompetent PCNSL typically occurs when the patient is approximately 58 years old, and is more frequent in men. Neuroimaging typically reveals a solitary lesion that is most commonly located within the basal ganglia or supratentorially in the white matter of the frontal or parietal lobes. On MRI, B-cell PCNSL lesions are clearly delineated masses that appear isointense to hypointense on T1-weighted images and mostly hypointense on T2-weighted images (**Fig. 4**). The short T2 hypointensity is related to a high nuclear-to-cytoplasmic ratio, which is characteristically seen with PCNSL.⁴⁸ Gadolinium enhancement is marked, homogeneous, and invariably present. These neoplasms are commonly seen within the corpus callosum and may “vanish” with steroids. In the case of PCNSL, corticosteroids not only reduce swelling but also cause tumor lysis, because they function as a chemotherapeutic agent.⁴⁹

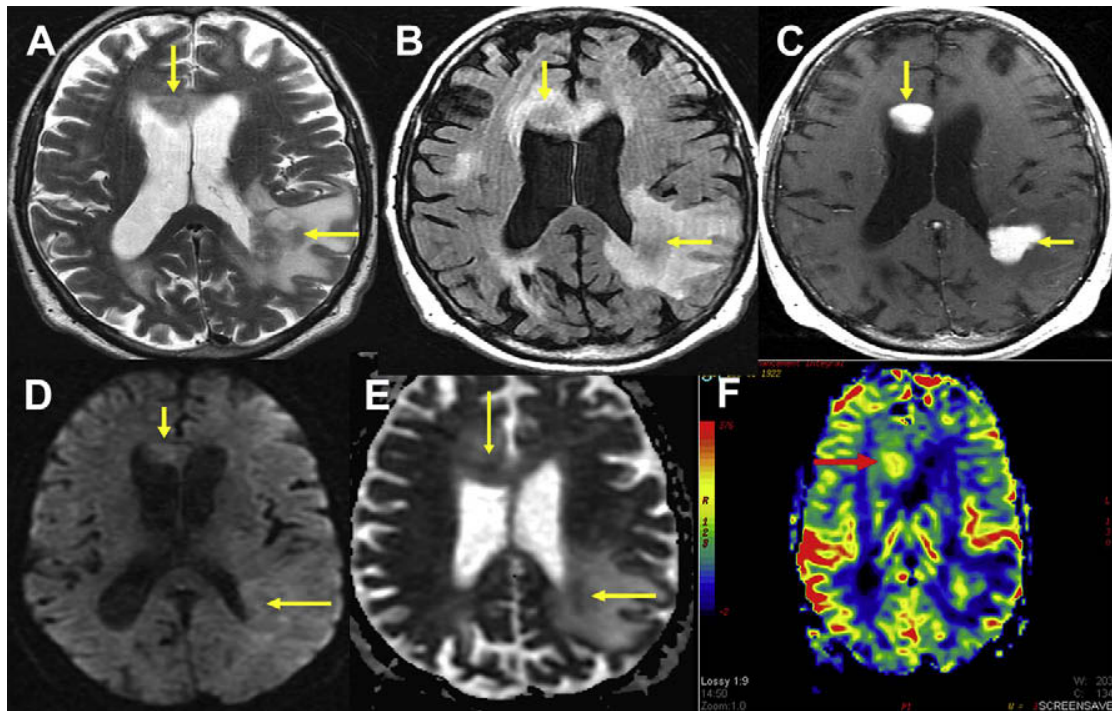


Fig. 4. The patient is a 75-year-old man with a 1-month history of rapidly progressive cognitive decline. Axial T2-weighted (A) and FLAIR (B) images show hyperintensities in a vasogenic pattern within the right frontal and left posterior frontal lobes. A relative hypointensity (short T2, *yellow arrows*), enhances vividly with gadolinium on the T1-weighted image (C). DWI MR (D) shows a relative hyperintensity (*arrow*), and the apparent diffusion coefficient map (E) reveals a hypointensity (*arrow*) consistent with relative restriction of proton diffusion, indicative of a high cytoplasmic-to-extracellular space ratio. PWI (F) confirms increased relative cerebral blood volume (*red arrow*) as expected in this patient who has a diagnosis of PCNSL.

PCNSL in immunocompromised patients is clearly different than in immunocompetent patients. Estimates indicate that nearly 6% of the AIDS population will be afflicted with PCNSL. Neuroimaging reveals a higher frequency of multiple lesions that are cortical based and more often display irregular margins, heterogeneity, hemorrhage, and ring enhancement, as compared with the findings in immunocompetent patients. An important dilemma in immunocompromised patients is the difficulty in distinguishing PCNSL from cerebral toxoplasmosis using CT and MRI, because both entities can present with multiple ring-enhancing lesions. Thallium single-photon emission CT or positron emission tomography (PET) can aid in this setting and should be considered before the empiric treatment of a presumed toxoplasmosis.^{50,51}

Meningiomas

Meningiomas are readily diagnosed by an extra-axial location on MRI and most often are an incidental finding. Fewer than 10% of meningiomas will ever cause symptoms, and these are the most common primary intracranial tumor (14%–20%), with a female preponderance. They occur most commonly in the 40- to 60-year-old range and are multiple in 1% to 9% of cases. Malignant and atypical meningiomas, although uncommon, account for approximately 7.2% and 2.4% of all meningiomas, respectively.⁵² They have less favorable clinical outcomes because they are more prone to recurrence and aggressive growth. Several key characteristic MRI signs include (1) having a CSF cleft sign between the tumor and brain (80% of cases), (2) buckling of the gray-white matter junction (3) involvement of the dura with a 40% to 60% incidence of the

“dural tail” sign, and (4) displacement of the pial vessels. Peritumoral edema may be evident, especially in symptomatic patients.⁵³ More than 95% of these tumors enhance homogeneously and intensely. GE sequences are the most sensitive for detection of the intratumoral calcification that occurs in one fourth of meningiomas.⁵⁴

NOVEL IMAGING IN NEURO-ONCOLOGY

Advances in MR spatial imaging techniques have yielded improvements in high-resolution anatomic imaging and in methods of evaluating physiology and function (**Box 2**). The following section is an overview of the current state of neuroimaging of brain tumors. It discusses three types of physiology-based MRI methods, namely, DWI, PWI, and pMRS.

Diffusion-Weighted Imaging

Molecular mobility of water molecules is the essential contrast mechanism exploited in DWI, reflecting a measurement of the apparent diffusion coefficient (ADC). The greater the density of structures impeding water mobility, the lower the ADC; therefore, ADC is considered a noninvasive indicator of cellularity or cell density. In the clinical practice of neurology, DWI has been used most commonly in the evaluation of acute ischemic infarctions.⁵⁵ In neuro-oncology, DWI has four important clinical applications. These include the assessment of (1) tumor differential diagnosis, (2) tumor grade and cellularity, (3) postoperative injury, and (4) integrity of white matter tracts.

Tumor differential diagnosis

DWI is used to differentiate between epidermoid cysts and arachnoid cysts. Both lesions present with similar T1 and T2 signal intensity, but on DWI, epidermoids are hyperintense.⁵⁶ Water molecules within arachnoid cysts have a high diffusibility, whereas they are restricted by keratinous debris within epidermoid cysts. Another important use of DWI is to differentiate a ring-enhancing GBM from an abscess. An abscess has a high signal on DWI and reduced ADC within the cavity. This restricted diffusion is thought to be related to the characteristics of pus within the cavity. On the other hand, necrotic and cystic tumors display a low signal on DWI with increased ADC and isointense or hypointense DWI signal intensity at the margin of the lesions.⁵⁷

The ADC of ependymomas is significantly lower than that of astrocytomas and may help in the differentiation of supratentorial ependymomas from grade 2 astrocytomas. In addition, the ADC of ependymomas is higher than that of medulloblastomas, which may also assist in differentiating posterior fossa fourth ventricular tumors.⁵⁸ Because PCNSL are hypercellular, so-called “blue cell” tumors, the ADC is, not unexpectedly, lower than that of other tumors such as GBM or metastases, which may aid in the differential diagnosis of enhancing periventricular masses. The ADC of meningiomas and schwannomas has been evaluated recently, and it was found that the ADC of schwannomas was significantly higher than that of meningiomas.⁵⁹

DWI can be used to differentiate cytotoxic edema from vasogenic edema. Vasogenic edema due to infiltrative gliomas and metastases is histologically different despite a breakdown in the blood–brain barrier seen in both. In GBM, the peritumoral edema is better referred to as infiltrative edema, because it represents vasogenic edema and infiltrating tumor cells.⁶⁰ DWI may be used to help differentiate between metastases and GBM on the basis of the ADC map of the surrounding edema. When peritumoral edema is due to neoplastic infiltration of a GBM, the ADC values tends to be lower compared with values related to the edema secondary to metastatic disease.⁶¹

Tumor grade and cellularity

With respect to gliomas, a recent study has found that the higher the tumor WHO grade, the lower the ADC.⁶² Free water diffusivity is restricted by hypercellularity. Smaller ADC values correspond with the most cellular tumor component, whereas larger ADC values are correlated with low cellularity. In patients who have malignant supratentorial astrocytomas, studies have shown that the pretreatment ADC is useful as a prognostic marker for survival.⁶³ DWI could also be used in assessment of response to therapy because of the universal relationship between ADC and cellular density, which suggests that the temporal evolution from viable tumor to treatment-induced necrotic tumor may be measurable by diffusion. Early increases in ADC values during therapy are hypothesized to relate to therapy-induced cellular necrosis, whereas a drop in ADC values within tumor compared with pretreatment levels is thought to be indicative of tumor regrowth (**Fig. 5**).

Postoperative injury

Reduced diffusion abnormality is not synonymous with acute cytotoxic edema. Any process that results in acute intracellular swelling and subsequent decrease in the surrounding extracellular space can lead to reduced diffusion in the brain. In the postoperative evaluation of brain tumors, restricted diffusion may represent areas of infarction, ischemia, traumatic surgical retraction, vascularity damage, tumor devascularization, and venous congestion secondary to acute cellular damage (**Fig. 6**).⁶⁴ Most areas of immediate postoperative diffusion abnormality invariably undergo a phase of contrast enhancement on routine anatomic images that can be easily misinterpreted as tumor recurrence. Regions of reduced diffusion after glioma surgery that show contrast enhancement on follow-up study may simulate the appearance of recurrent tumor. These areas of enhancement invariably evolve into encephalomalacia or a gliotic cavity on long-term follow-up studies, as one would expect in a region of permanent brain injury.⁶⁵

DWI may also assist in differentiation of recurrent tumor from radiation injury. Newly enhancing lesions that arise on routine follow-up brain MRI at the site of previously treated primary neoplasm represent a diagnostic dilemma. ADC values in tumor recurrence are significantly lower than those occurring with treatment-related changes, such as radiation necrosis.⁶⁶

Integrity of white matter tracks

Radiotherapy treatment planning for high-grade gliomas is also hampered by the ability to image peritumoral white matter infiltration. DWI sequences have been adapted to perform diffusion tensor imaging (DTI) by acquiring data in six or more directions. A tensor is used to describe diffusion in an anisotropic system. DTI allows us to visualize the location, orientation, and anisotropy of the brain's white matter tract. It can be used to provide maps of white matter fiber tracts (tractography) in brain tissue adjacent to tumors.⁶⁷ DTI tractography maps of desired white matter tracts (ie, corticospinal tract) can be overlaid onto high-resolution⁶⁸ T1-weighted images and provide information on alterations in fiber tract directionality and integrity due to neighboring brain tumor. By elucidating the anatomic relationship of motor and sensory pathways to tumor tissue, DTI has the potential to reduce surgical morbidity.^{69,70}

Conventional anatomic MR images have failed to identify tumor margins on T2-weighted images. In 40% of cases, tumor infiltration occurs in brain that appears normal on T2-weighted images.⁷⁰ DTI reveals larger peritumoral abnormalities in gliomas that are not apparent on conventional MRI. These abnormalities seem to precede the development of gross tumor recurrence on follow-up imaging.⁷¹ Through its ability

Box 2**Advanced MRI in neuro-oncology***Diffusion-weighted imaging (plus apparent diffusion coefficient)*

Scan time^a: 1 minute

Indications:

- A. Grading of tumor cellularity
 - Low-grade versus high-grade glioma
- B. Differential diagnosis.
 - 1. GBM versus abscess versus Multiple Sclerosis
 - 2. Primitive neuroectodermal tumor versus ependymoma
 - 3. Meningioma versus schwannoma
 - 4. Arachnoid versus epidermoid cyst
- C. Peritumoral edema of metastases versus GBM
- D. Define extent of tumor for biopsy and resection
- E. Assessment of tumor response.

Diffusion tensor imaging

Scan time^a: 5 ½ minutes

Indications:

- A. Preoperative assessment of white matter tracts for surgical guidance
- B. Prediction of postoperative dysfunction
- C. Radiotherapy planning

Dynamic susceptibility contrast MRI (relative cerebral blood volume)

Scan time^a: 60 seconds (4 minutes for high resolution three dimensional)

Indications:

- A. Low-grade versus high-grade tumor
- B. Define aggressive tumor extent for biopsy and resection
- C. Radiation necrosis versus recurrence
- D. Response to treatment

Dynamic contrast-enhanced MRI (endothelial permeability)

Scan time^a: ~5 minutes

Indications:

- A. Low-grade versus high-grade tumor
- B. Define aggressive tumor extent for biopsy and resection
- C. Radiation necrosis versus recurrence
- D. Response to treatment

MR spectroscopy

Scan time^a: 8 minutes (typically 2 samples at 4 minutes each)

Indications:

- A. Grading gliomas
- B. Expanding differential diagnosis
 - 1. Radiation necrosis versus recurrence
 - 2. Peritumoral edema of metastases versus GBM
 - 3. Neoplasm versus abscess versus Multiple Sclerosis
 - 4. Confirm meningioma

Chemical shift imaging

Scan time^a: 10 minutes

Indications:

- A. Multivoxel MR spectroscopy to help surgeon in the extent of surgery and biopsy sight
- B. Predict radiotherapy fields
- C. Monitor response to treatment

Functional MRI

Scan time^a: 4 minutes (per functional assessment).

Indications:

- A. Mapping eloquent areas of the brain pre-operatively
- B. Evaluation of speech dominance (Wada test)
- C. Selection for intraoperative cortical stimulation
- D. Guidance for neuronavigation

^a Typical for 3-tesla MRI system. Resolution, scan time, or image quality degrade at 1.5 tesla.

to detect infiltration, DTI may allow triage of patients among aggressive therapy, standard treatment, and palliative care. In addition, it can improve the delineation of radiation therapy target volume and potentially direct DTI-targeted stereotactic biopsies.⁷²

Perfusion-Weighted Imaging

PWI measures the degree of tumor angiogenesis and capillary permeability, both of which are important biologic markers of malignancy, grading, and prognosis, particularly in gliomas. Various PWI methods can be used to study and quantify brain tumor vasculature and the following section will focus on the three most widely used methods.⁷²

Dynamic susceptibility contrast (DSC) MRI is a technique that uses rapid echo-planar imaging measurement of T2- or T2*-weighted signal changes after an injection of a bolus of a compound such as gadolinium. It relies on the T2* signal drop caused by the passage of gadolinium-containing contrast agent through the tissues. The drop in signal is proportionate to the concentration of the contrast agent and the tissue vascularity. The most robust quantitative variable derived is relative cerebral blood volume (rCBV), which represents tumor angiogenesis. Cellular studies have demonstrated a strong positive correlation among tumor, rCBV, and astrocytoma grading.

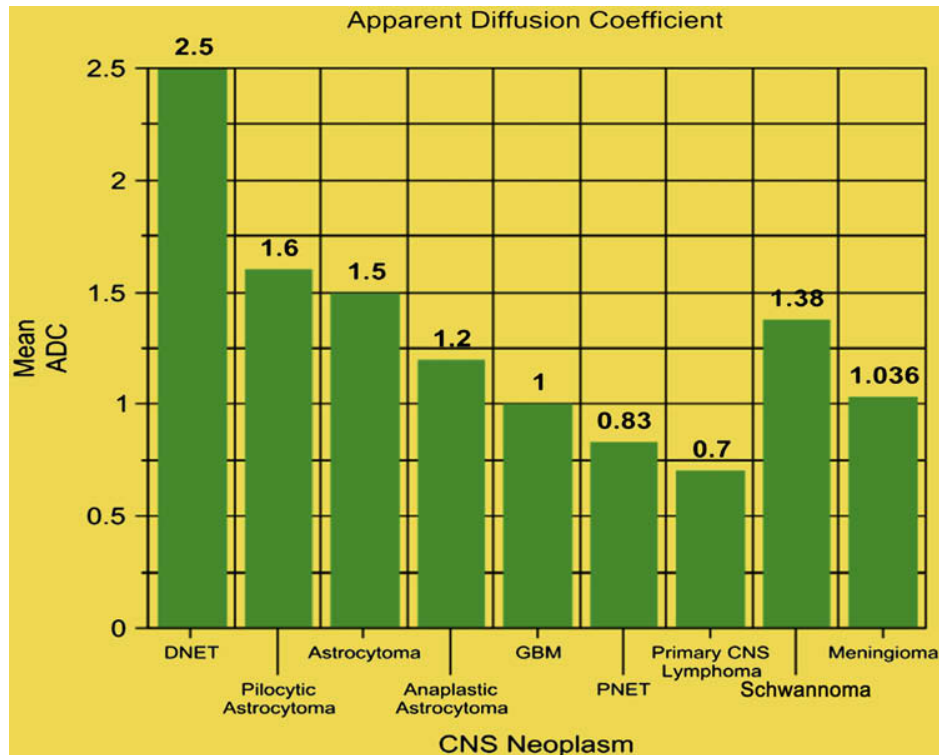


Fig. 5. The use of the ADC in the differentiation of brain neoplasms. ADC is especially useful for astrocytic tumors, WHO II-IV. DNET, dysembryoplastic neuroectodermal tumor; PNET, primitive neuroectodermal tumor.

Low-grade astrocytomas have significantly lower average rCBV than AA or GBM. rCBV maps may be used to select biopsy sites for enhancing and nonenhancing tumors by highlighting the “hot” area for surgery.⁷³

Nonastrocytic gliomas, most notably oligodendrogliomas,⁷⁴ are a more heterogeneous group with respect to rCBV. They may have high rCBV, even in low-grade tumors. With DSC MRI, lymphomas tend to show elevated rCBV but not to the same degree as in GBM,⁷⁵ likely because florid angiogenesis is not a typical feature of PCNSL. Meningioma is a highly vascular tumor that usually derives blood supply from the dural vessels of the external carotid artery, although pial supply is not uncommon.⁷² DSC MRI-derived rCBV measurements of meningiomas may be grossly overestimated or underestimated because of the leakage phenomenon during the first pass.^{63,76} Metastatic brain tumors contain capillaries that are highly leaky, but the rCBV is similar to that of GBM; however, the rCBV within peritumoral edema is higher in GBM than in solitary metastasis.⁷⁷

A second type of PWI is called *dynamic contrast enhancement* (DCE). DCE MRI consists of repeated imaging with a T1-weighted sequence and provides information about endothelial permeability. A pharmacokinetic compartmental model enables the concentration of gadolinium in tissue to be calculated as a function of time after bolus injection of the contrast agent. This technique may be used for studying the microcirculation of tumors. Using DCE MRI rather than DSC MRI has a clear advantage. The former offers better spatial resolution, reasonable imaging time, and resistance to susceptibility artifact; however, DSC is currently technically more reliable than DCE.⁷⁸

The third type of technique is called *arterial spin labeling*. This technique uses an endogenous contrast mechanism in which blood flowing into the brain is labeled by the MR system itself. Because it requires no contrast agent administration, it is completely non-invasive and repeatable. Regional flow distributions can be assessed independently. In

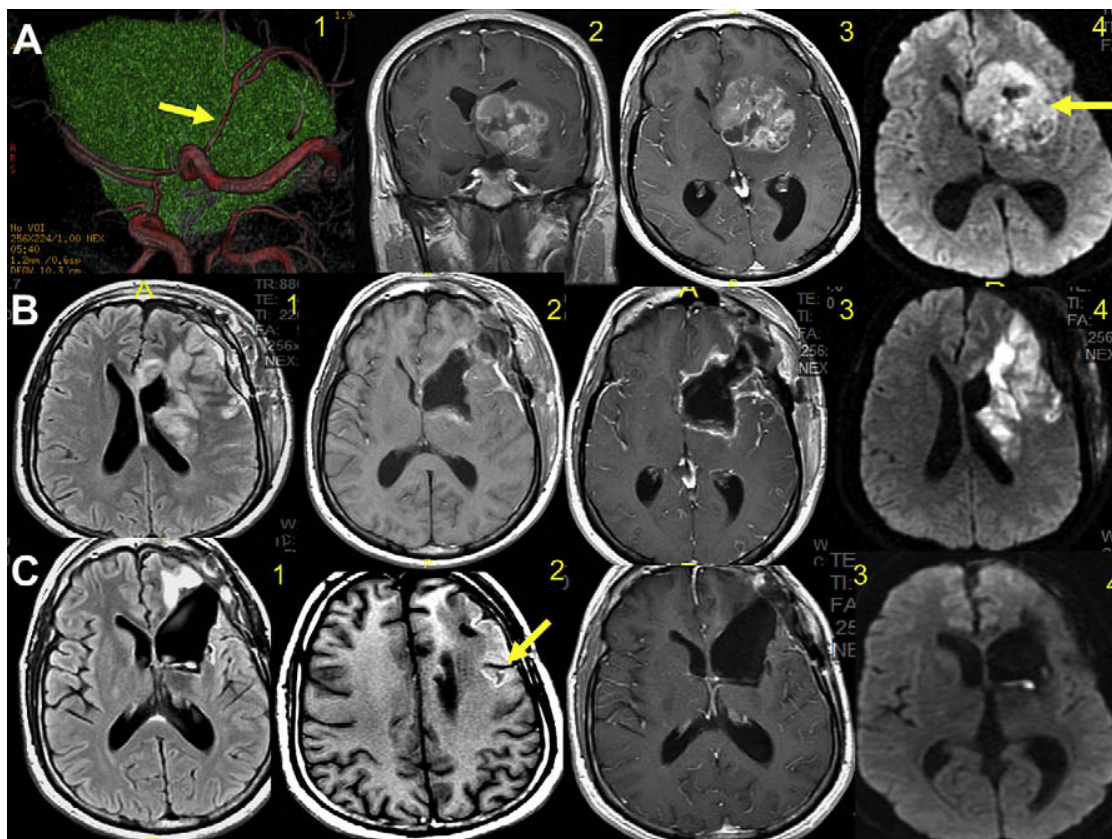


Fig. 6. The patient is a 26-year-old man who presented with right hemiparesis and word-finding difficulties and was found to have a large mass within the deep left frontal lobe. On the three-dimensional MR angiography reconstruction image (A1), the tumor (green) is bordered medially by the anterior cerebral artery and a thinned (arrow) middle cerebral artery (red). T1-weighted coronal (A2) and axial (A3) contrast images show a large, irregular, enhancing, and necrotic mass compressing the adjacent lateral and third ventricles. With DWI (A4), the tumor is hyperintense (arrow), indicative of hypercellularity, consistent with a GBM. Five days after a debulking surgical procedure in which intraoperative MRI was used, the patient's symptoms worsened. FLAIR image (B1) shows significant hyperintensities involving the cortex and subcortical white matter of the left frontal lobe. T1-weighted axial images without (B2) and with (B3) contrast show an extensive postoperative cavity. (B4) DWI shows extensive restricted diffusion in the left frontal lobe. One month after surgery, FLAIR image (C1) shows less mass effect and resolving hyperintensities. T1-weighted noncontrast study (C2) shows a hyperintensity in a gyral pattern most consistent with petechial hemorrhage (arrow). Contrast MRI (C3) confirms a lack of enhancement consistent with gross total resection. DWI (C4) is unremarkable. The patient's weakness and dysphasia gradually resolved. The most likely explanation for these imaging findings is postoperative left middle cerebral artery vasospasm with ischemic tissue that did not evolve into a completed infarction because of cortical reperfusion.

addition, truly quantitative values of cerebral blood flow can be obtained.⁷⁹ This promising technique is beginning to move out of the research realm and into clinical practice.

In summary, PWI has been used to characterize glioma WHO grade and tumor genotype, guide biopsy, and provide prognostic information.^{74,80} Thus, PWI together with conventional MRI should be considered in the diagnosis and monitoring of brain tumors before, during, and after therapy. PWI can easily be incorporated into the routine clinical evaluation of intracranial mass lesions because of the short imaging and data processing times and the use of a standard dose of contrast agent. In addition, DCE MRI techniques provide complimentary functional information along with high resolution of structural information.

Proton MR Spectroscopic Imaging

MRS is a powerful noninvasive imaging technique that offers metabolic information on brain tumor biology that is not available from anatomic imaging. This subject has been reviewed by Dr. Ross in this edition of *Neurologic Clinics*; however, a summary as it pertains to CNS neoplasms will be discussed. In high-grade gliomas, the characteristic spectroscopic appearance demonstrates an increase in choline (Cho) peak, a decrease in the *N*-acetyl aspartate (NAA) peak, an increase in the Cho-to-creatinine ratio, and, in some cases, the presence of a lactate peak. Potential uses of pMRS include refinement of preoperative differential diagnoses, biopsy site selection, monitoring of response to treatment, and distinction of progressive tumors from treatment effects (**Box 3**). Furthermore, a derivative imaging technique has been developed called chemical shift imaging, in which metabolic data yielded by spectroscopy are overlaid on high-resolution T1- or T2-weighted images.⁸¹

The metabolites responsible for the NAA signal are predominately found in neurons; thus, reduction in this signal in neoplasms arises from reduced or absent production of these metabolites because normal neurons have been destroyed or displaced by a neoplastic process. The current view is that the elevated Cho peak is a surrogate marker of increased cell membrane turnover caused by tumor growth or normal cell destruction. However, an alternate view suggests that the Cho signal may, at least in part, be elevated because of increased production through phospholipase up-regulation. The relative anaerobic environment of many neoplasms causes derangements in glucose metabolism, which results in incomplete glucose breakdown and likely accounts for the elevated lactate signal.⁸²

Box 3

Potential applications for proton MR spectroscopic imaging in neuro-oncology

Preoperative

- Differentiate high-grade from low-grade gliomas
- Differentiate GBM-tumor edema from metastases-related edema
- Refine preoperative differential diagnosis
 - Abscess
 - Tuberculoma
 - Tumefactive demyelinating lesion

Diagnose meningioma

Diagnose CNS lymphoma

Perioperative

- Localize stereotactic biopsy
- Determine extent of resection
- Multivoxel pMRS to predict radiotherapy volumes

Postoperative

- Monitor malignant transformation of low-grade tumors
- Monitor response to treatment
- Differentiate recurrent GBM from radiation necrosis

pMRS in neuro-oncology may be used preoperatively in differentiating between neoplastic and nonneoplastic disease and grading and expanding differential diagnoses.⁸³ In regard to guidance for therapy, it may be used in determining the extent of resection and biopsy site choice. Multivoxel pMRS has been used for radiation planning instead of T1-weighted gadolinium contrast or T2-weighted images. It may also be used for assessment and treatment efficacy and response with radiation or chemotherapy. pMRS has been used to evaluate low-grade tumor malignant transformation and to differentiate radiation necrosis from recurrent tumor.⁸⁴ Multivoxel pMRS improves the imaging of brain tumors because it not only enables biochemical assessment of tumor dynamics, but also depicts residual or recurrent tumor outside the gadolinium-enhanced tumor bed (Fig. 7).^{85,86}

NEUROIMAGING OF TUMOR RESPONSE

Imaging of tumor response to treatment has clinically meaningful end points for patients who have brain tumors, which includes overall survival, progression-free

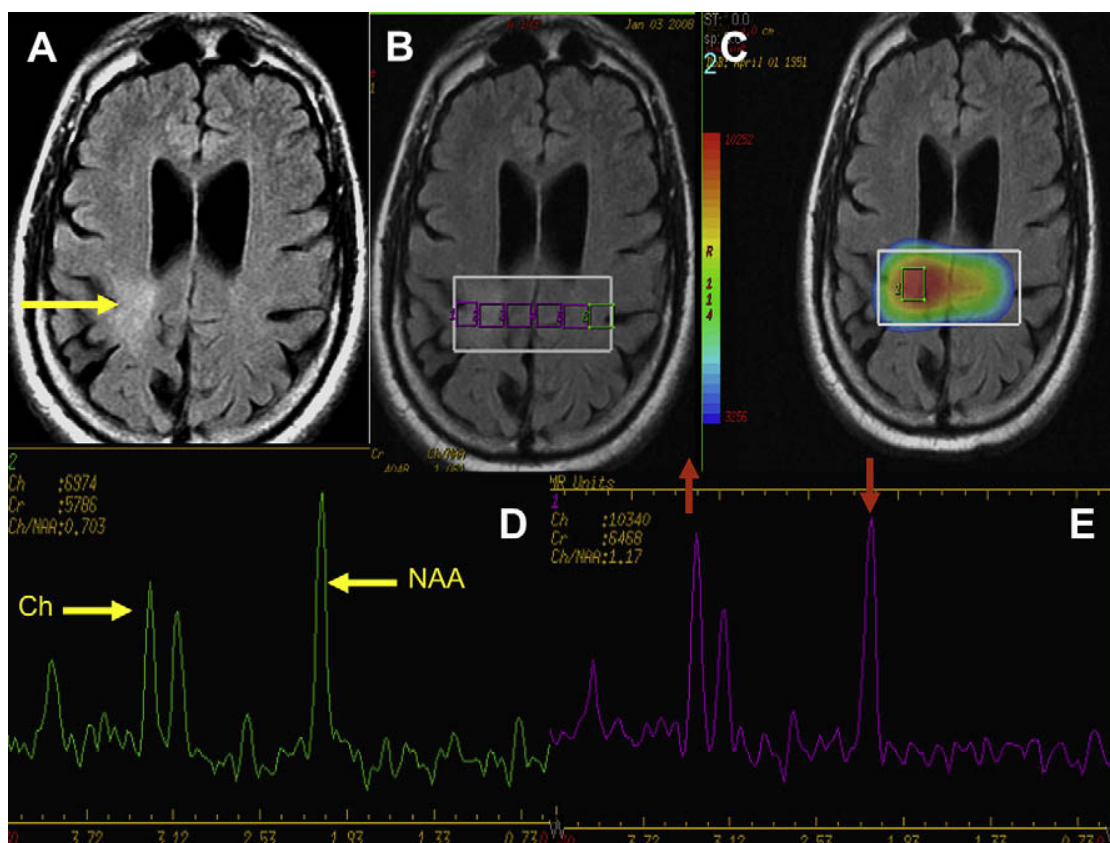


Fig. 7. The patient is a 30-year-old man with left-sided numbness. FLAIR (A) confirms a vague area of hyperintensity within the right posterior frontal lobe (arrow). Multivoxel pMRS (B) confirms a slight decrease in NAA and an increase in Cho (area in rectangle), consistent with a low-grade astrocytoma. Chemical shift imaging (C) allows neurosurgeons to biopsy nonenhancing tumors in the region where the Cho peak is the highest (area in rectangle), which, in turn, represents the most hypercellular component of the tumor. In addition, the radiation oncologist may use the findings on chemical shift imaging to fine-tune the radiation field to include not only the T2 hyperintensity but also the Cho map. The pMRS (D, green) of the normal brain shows a typical pattern, with the highest peak at 2.0 parts per million, representing NAA (arrow pointing left) and the second highest peak Cho (arrow pointing right) at 3.2 parts per million. Within the biopsy-proved astrocytoma (WHO II), the pMRS (E, purple) confirms a relative increase in Cho (red up arrow) and decrease in NAA (red down arrow).

survival, and time to progression. In addition to this, radiographic response is used in the evaluation of brain tumor response in large clinical studies. Gadolinium enhancement is measured as a response in most clinical trials; however, gadolinium enhancement does not measure nonenhancing tumors. This approach tends to measure vascular permeability due to a breakdown in the blood–brain barrier rather than tumor. Factors such as radiation damage and use of glucocorticoids or vascular-stabilizing drugs can affect vascular permeability. The two major approaches that are available for the evaluation of contrast-enhancing tumor and T2-weighted nonenhancing infiltrative tumor in serial imaging studies during clinical trials are (1) diameter-based measurement on a single axial section containing the largest diameter of tumor (response evaluation criteria in solid tumors [RECIST] or MacDonald criteria) and (2) computer-assisted volumetric analysis of all sections containing tumor.^{87–89}

Among the diameter methods, the two most commonly used are the measurement of the single largest diameter (one-diameter or RECIST) or the orthogonal diameters (two-diameter or MacDonald criteria) on a single axial section.^{88,89} RECIST has not been widely adopted for clinical trials involving brain tumors mainly because of the historic use of two-diameter criteria. RECIST measures the longest single linear-enhancing diameter across a lesion in the axial plane. When multiple lesions are analyzed, the individual diameter measurements are recorded separately and are then summed for response evaluation. In the MacDonald criteria, a measurement is made of the maximal enhancing tumor diameter on a single axial gadolinium-enhanced T1-weighted section. The largest perpendicular diameter is measured on the same image. The product of the two diameters is calculated, and the measurements are repeated for each scan. Computer-aided volumetric methods are more labor intense and are not done routinely in the evaluation of brain tumors in clinical studies. Correlation between quantitative parameters of response criteria between RECIST to MacDonald and volumetric approach have not been examined closely.⁹⁰

Some complicating factors in postoperative brain tumor imaging are that areas of restricted diffusion along the margin of the surgical cavity are present on DWI in up to two thirds of patients on immediate postoperative scans following surgery for malignant gliomas and usually represent areas of infarction. In approximately one half of these cases, enhancement lasts for a period of 1 to 2 weeks after surgery, a finding that is often misinterpreted as progressive tumor. Thus, it is important to obtain and review the immediate postoperative DWI when new enhancement appears within 2 to 4 weeks of surgery.⁹¹ Optimal postoperative imaging includes an MRI study that is acquired within 72 hours following surgery to minimize postoperative enhancement along the margin of the surgical cavity. The use of 3-mm, skip 0-mm T1-weighted gadolinium contrast-enhanced images improves resolution, particularly when dealing with smaller enhancing nodules. Although obtaining these high-resolution images increases acquisition time, the improvement of resolution is a strong argument in favor of this form of imaging. The dose of gadolinium should always be documented and similar in each successive study. Postcontrast multiplanar images should be acquired at a standardized time after gadolinium injection, starting no less than 5 minutes after injection. When using 3-T MRI, it is time effective to obtain a single three-dimensional volume before and after contrast administration; orthogonal image planes can then be reconstructed rather than directly acquired. Other sequences not affected by gadolinium, such as T2-weighted images and DWI, can be routinely acquired after contrast injection to optimize scanner resources.

The use of T1-weighted gadolinium enhancement is the most useful sequence for the measurement of brain tumors, although recently, some confusion has occurred with newer forms of brain tumor treatment. Such treatment specifically includes monoclonal antibodies that inhibit vascular endothelial growth factor, such as

bevacizumab. Bevacizumab produces a rapid decrease in the degree of contrast enhancement within malignant gliomas and the extent of surrounding hyperintense T2-weighted signal intensity. This finding is consistent with a decrease in the permeability of the blood–brain barrier and makes it difficult to use conventional measures of tumor size in the setting of clinical trials, which is one of the reasons why it is important to incorporate advanced techniques, such as perfusion and permeability imaging, and pMRS. In the future, we will be looking not only at anatomic changes but also at biologic or so-called metabolic changes in the brain in response to treatment.⁹²

FUNCTIONAL MRI

In the field of neuro-oncology, one of the driving dictums of neurosurgical intervention is maintaining the quality of life postoperatively in patients who have infiltrating tumors. We know today that more aggressive neurosurgical resection results in less residual tumor, increased patient survival, and improved quality of life. Functional MRI (fMRI) is a neuroimaging method that is able to depict not only the detailed anatomy of the brain but also brain function, in a noninvasive manner.⁹³ When an area of the brain is metabolically active, blood flow increases correspondingly. The increased blood flow is not matched by an increase in oxygen extraction, so the concentration of deoxyhemoglobin is reduced. Because deoxyhemoglobin is paramagnetic, the T2* weighted signal changes. This change, referred to as blood oxygen level–dependent contrast (BOLD), is detected by the MRI sequence. fMRI has moved from the research environment into clinical neuro-oncologic practice and is used primarily for preoperative localization of eloquent brain regions before tumor resection, in an attempt to minimize intraoperative morbidity (**Fig. 8**). fMRI reliably localizes the primary motor and sensory areas of the cortex. Furthermore, the ability to identify speech areas reliably may make the Wada test for speech and memory laterality obsolete.⁹⁴

Four goals of presurgical fMRI include (1) determining the feasibility of surgical treatment and risk for inducing neurologic deficits, (2) selecting patients for intraoperative cortical stimulation,⁹⁵ which would be indicated when a functional area is included within the lesion or at the radiologic boundary, (3) providing guidance for functional neuronavigation based on preoperatively acquired structural information using MRI,^{96,97} and (4) shortening the operative time under anesthesia. Compared with PET, cortical stimulation, and magnetoencephalography techniques for imaging brain activity, fMRI requires no radioactive isotope, short total scan time (1–4 minutes per run), and high resolution of approximately 1.5 mm × 1.5 mm.

HIGH-FIELD MRI

The Food and Drug Administration has approved a magnet of up to 8.0 tesla (T) for imaging in humans. A 9.4-T magnet, which has a magnetic field that is approximately 100,000 times stronger than the earth, is being used in human scanning at the University of Illinois at Chicago. The magnet is surrounded by 520 tons of steel that block its magnetic field. Currently, imaging up to 4.0 T is available for clinical practice. Ultra-high-field MRI generally refers to imaging at a field strength of 7.0 T or more. Presently, 1.5-T MR systems are considered midfield, and 3-T systems are considered high field.⁹⁸ Three-tesla scanners are considered currently to be the state-of-the-art imaging modality for CNS diseases. At 3 T, the signal-to-noise ratio increases approximately twofold compared with 1.5 T. Using techniques such as parallel imaging, this increased signal-to-noise ratio can be traded in for improved resolution and reduction in acquisition time. In parallel imaging, different elements in the receiver coil array simultaneously sample the MR signal from the same anatomy; these independent

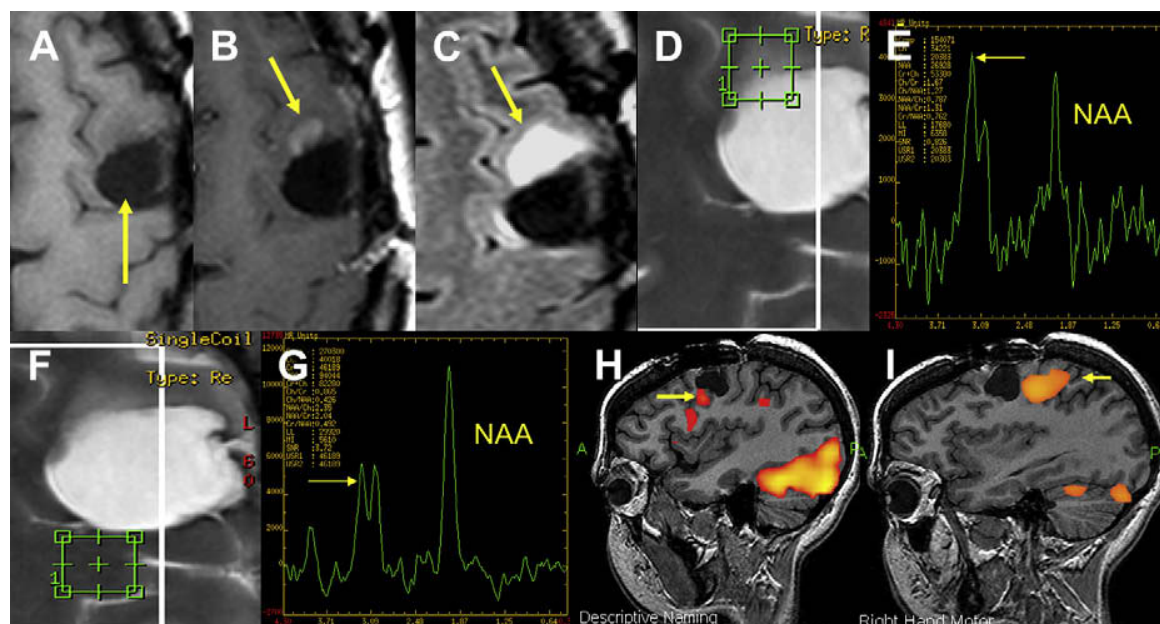


Fig. 8. The patient is a 31-year-old woman who had had an operation 1 year previously for an oligoastrocytoma located in the superior aspect of the left middle frontal gyrus. Routine follow-up T1-weighted image (A) obtained using a 3.0-T magnet confirms a postoperative cavity (arrow), although contrast T1-weighted image (B) shows a new area of enhancement just anterior to the cavity (arrow). FLAIR (C) shows an enlarging area of hyperintensity or long T2 (arrow). Preoperative pMRS (D, E) shows a decrease in NAA and an increase in CHO peak (arrow) in the area of progression, consistent with tumor recurrence. When the voxel is placed posterior to the cavity, the pMRS is normal (F, G). Functional MRI in the sagittal plane using descriptive naming (H) indicates activation in the left premotor cortex just below the enhancing lesion (arrow). For right-hand movement, activation (I) was found adjacent to the posterior margin of the postoperative cyst that was found to be normal on pMRS. These test results aided the neurosurgeon in the resection of the enhancing lesion and adjacent T2-weighted hyperintensities without postoperative residual neurologic deficits. The pathology was consistent with an anaplastic astrocytoma.

geometric views are used to reduce the number of repetitions normally required to produce a desired resolution. The speed-up factor in parallel imaging is referred to as the SENSE factor.⁹⁹ Increased SENSE factors can also be used to reduce echo-planar imaging artifacts. For example, using an eight-channel phased-array coil with SENSE, rather than conventional quadrature coil imaging, significantly improves the quality and usefulness of DSC PWI at 3 T.¹⁰⁰

Brain tumors have been studied with contrast-enhanced MRI at 3 T compared with 1.5 T. The advantages of 3 T include larger effect of paramagnetic contrast agents. At 3 T, one half the dose of contrast agent is needed, compared with 1.5 T.¹⁰¹ In addition, with brain tumors, lesion-to-brain contrast-to-noise ratio at 3 T is increased twofold when compared with 1.5 T. Major advantages with 3 T include the fact that this higher field yields a better BOLD response for fMRI, more signal, and better dispersion of peaks, which improves the quality and specificity of MR spectroscopy. The image quality of patients needing spine imaging and MR angiography or venography is also improved.

Ultra-high-field MRI is associated with greater sensitivity to susceptibility contrast. MR GE pulse sequences, such as susceptibility-weighted imaging (SWI), allow good visualization of microvasculature, especially the neovasculature that is found in high-grade brain tumors. SWI is a high-spatial-resolution three-dimensional GE MRI technique with phase postprocessing that accentuates the paramagnetic properties of blood products such as deoxyhemoglobin, intracellular methemoglobin, and

hemosiderin¹⁰² SWI can increase the visibility of tumors and is helpful for depicting hemorrhage, calcification, and increased vascularity in some neoplasms, which may reflect tumor grade. Iron and calcium can be discriminated on the basis of their paramagnetic versus diamagnetic behavior on SWI, which may help differentiate tumors that are more prone to calcify, such as oligodendrogliomas. Aggressive tumors tend to have rapidly growing vasculature and many microhemorrhages; hence, the ability to detect these changes in the tumor could lead to better determination of the tumor's biologic behavior. Undoubtedly, clinicians and researchers suffer from so-called "Tesla envy" but, despite the increased cost and, at times, the technical difficulties, the future undoubtedly will progress to stronger magnets and improve the resolution and functional imaging of brain tumors.

INTRAOPERATIVE MRI

Neuronavigation systems improve lesion targeting and resection of tumor tissue while optimizing minimally invasive surgical techniques (Fig. 9). Frame-based and frameless stereotactic systems rely on preoperatively obtained MRI or CT data and will inevitably suffer from diminished accuracy as the duration of the surgical procedure increases. Unfortunately, neuronavigation systems do not allow the neurosurgeon to adjust for dynamic changes that occur intraoperatively, such as brain shift. In addition, it is difficult at times to define the margins of low-grade infiltrative gliomas by visual inspection and also to identify potential complications that occur outside the surgical field.^{103,104}

Intraoperative MRI surgical suites have been operational for more than 15 years. Field strengths for these intraoperative MRI systems have ranged from 0.1 to 3 T.¹⁰⁵ The main advantages of intraoperative MRI are its excellent soft-tissue discrimination and three-dimensional visualization of the operative site, and its near real-time imaging to evaluate the extent of tumor resection or hemorrhage, minimize scalp incision and craniotomy site with preoperative imaging, and immediately assess intraoperative brain shift.¹⁰⁶

The advantage of high-field intraoperative MRI systems is the inclusion of functional capabilities such as pMRS, fMRI, MR venography, MR angiography, chemical shift imaging, and DWI. The use of intraoperative MRI has led to advances in the extent of tumor resection. In addition, GE sequences with long echo times (ie, 40–60 milliseconds) show dark signal ("blooming") due to hyperacute blood collections, which helps in the imaging of postoperative bleeds. Intraoperative MRI is approaching the point

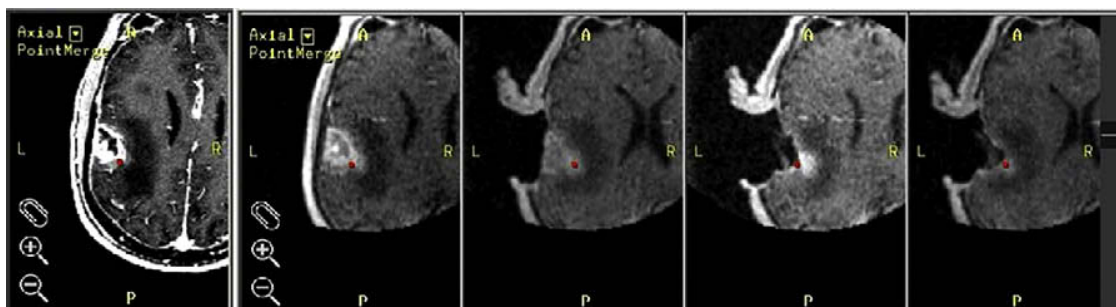


Fig. 9. Intraoperative MRI of a GBM resection in a 45-year-old woman presenting with left-sided weakness. Postoperatively, the patient had gross total resection of the contrast-enhancing lesion without significant morbidity. (A) Preoperative T1-weighted gadolinium contrast study showing a necrotic mass within the posterior frontal lobe on the right. (B) Initial intraoperative MRI. (C, D, and E) Time-dependent T1-weighted contrast images taken during surgery.

where it will be used not only to localize the target and guide the resection of brain tumors and other intracranial lesions but also to provide a comprehensive picture of surrounding functional anatomy with fMRI.¹⁰⁷

In addition to this, MRI-guided focused ultrasound surgery, which is noninvasive thermal ablation of tumors that is monitored and controlled by MRI, is currently being studied, with encouraging results.¹⁰⁸ By combining focused ultrasound with MRI-based guidance and control, it may be possible to achieve complete tumor ablation without any associated structural injury or functional deficit. Moreover, focused ultrasound can be used selectively to open the blood–brain barrier without damaging the surrounding brain parenchyma,¹⁰⁹ which is achieved by injecting preformed gas bubbles into the vasculature, as it is done routinely with transcranial Doppler. The gas bubbles implode and release cavitation-related energy, which transiently opens the tight junctions. Large molecules, such as chemotherapeutic or neuropharmacologic agents, may pass through this artificially created “window” in the blood–brain barrier.

MOLECULAR IMAGING

Molecular imaging provides information regarding diseases at the biochemical and genetic levels, which potentially will be more precise and specific than anatomic and physiologic methods. This rapidly emerging sphere of investigation seeks to achieve imaging of molecular processes within brain tumor cells *in vivo*. MR images now give us insights into the physiology of human tumors in a way that is noninvasive and radiation free. The role of anatomic imaging will remain undisputed for planning of surgery and biopsy, but molecular imaging will assume the crucial role of response prediction and treatment monitoring.

Paramagnetic chelates that can change their magnetic properties on enzymatic hydrolysis are under investigation. Magnetic nanosensors are being developed and might be able to detect specific DNA or RNA sequences. Tumor cell–specific uptake of monocrySTALLINE iron oxide nanoparticles can be achieved because of the high concentration of transferrin receptors on the cells. Thus, these tumor cells have a high rate of endocytosis of the nanoparticles and they can be imaged with MRI.¹¹⁰

In recent years, molecular imaging of angiogenesis has become one of the most important studied areas of cancer research. Angiogenesis is fundamental in various physiologic and pathologic processes.¹¹¹ The ability to visualize and quantify angiogenesis will allow early diagnosis and monitoring for clinical determination of angiogenesis states before, during, and after antiangiogenic and therapeutic treatment. A novel method for direct imaging of angiogenesis used in MRI involves intravenous infusion and tracking of the subsequent migration of labeled endothelial precursor cells into tumors. Approximately 9 days after infusion, hypointense regions on GE images consistent with cell migration of tumor vasculature can be seen.^{112,113}

SUMMARY

Neuroimaging is now entering a more mature era whereby we can ask sophisticated questions concerning the biologic behavior of brain tumors. The shift from anatomic imaging to functional and molecular imaging has been evident over the last several years. Multimodality imaging (CT, MR, PET, and ultrasound) offers the most precise information noninvasively on tumor type and grade, guides therapeutic choices, and assesses the effects of therapy. Hence, imaging protocols need to be standardized across neuroimaging centers and measured parameters need to be defined and validated. The incorporation of fMRI (such as DWI, DTI, pMRS, and PWI) as part of

the mainstream clinical imaging protocol has allowed neuro-oncologists a window of opportunity to assess the biologic behavior of brain neoplasms. Future research will attempt to integrate multimodality approaches arising from the realization that distinct physiologic mechanisms underlie the signal generation for different imaging modalities. These novel approaches will eventually be routinely used preoperatively, intraoperatively, and eventually, therapeutically.

REFERENCES

1. CBTRUS. Statistical report: primary brain tumors in the United States 2000–2004. Central brain tumor registry of the United States data 2000–2004. Available at: www.cbtrus.org/reports/reports.html.
2. Jemal A, Siegal R, Ward E, et al. Cancer statistics 2007. *CA Cancer J Clin*. 2007; 57(1):43–66.
3. Buckner JC, Brown PD, O'Neill BP, et al. Central nervous system tumors. *Mayo Clin Proc* 2007;82(10):1271–86.
4. Terae S, Yoshida D, Kudo K, et al. Contrast-enhanced FLAIR imaging in combination with pre- and postcontrast magnetization transfer T1-weighted imaging: usefulness in the evaluation of brain metastases. *J Magn Reson Imaging* 2007;25:479–87.
5. Thomas B, Krishnamoorthy T, Kapilamoorthy T, et al. Contrast enhanced FLAIR imaging in ibuprofen induced aseptic meningitis. *Eur J Radiol Extra* 2006; 60(3):97–9.
6. Husstedt HW, Sickert M, Kostler H, et al. Diagnostic value of the fast-FLAIR sequence in MR imaging of intracranial tumors. *Eur Radiol* 2000;10(5):745–52.
7. Essig M, Hawighorst H, Schoenberg SO, et al. Fast fluid-attenuated inversion-recovery (FLAIR) MRI in the assessment of intraaxial brain tumors. *J Magn Reson Imaging* 1988;8(4):789–98.
8. Delfaut EM, Beltran J, Johnson G, et al. Fat suppression in MR imaging: techniques and pitfalls. *Radiographics* 1999;19(2):373–82.
9. Bauer-Melnyk A, Buhmann S, Becker C, et al. Whole-body MRI versus whole-body MDCT for staging of multiple myeloma. *AJR Am J Roentgenol* 2008; 190(4):1097–104.
10. Chan MS, Roebuck DJ, Yuen MP, et al. MR imaging of the brain in patients cured of acute lymphoblastic leukemia—the value of gradient echo imaging. *AJNR Am J Neuroradiol* 2006;27(3):548–52.
11. Patel MR, Siewert B, Klufas R, et al. Echoplanar MR imaging for ultra-fast detection of brain lesions. *AJR Am J Roentgenol* 1999;173:479–85.
12. Knauth M, Forsting M, Hartmann M, et al. MR enhancement of brain lesions: increased contrast dose compared with magnetization transfer. *AJNR Am J Neuroradiol* 1996;17:1853–9.
13. Finelli DA, Hurst GC, Gullapali RP, et al. Improved contrast of enhancing brain lesions on postgadolinium, T1-weighted spin-echo images with use of magnetization transfer. *Radiology* 1994;190(2):553–9.
14. Lee JM, Jung S, Moon KS, et al. Preoperative evaluation of venous systems with 3-dimensional contrast-enhanced magnetic resonance venography in brain tumors: comparison with time-of-flight MRV and digital subtraction angiography. *Surg Neurol* 2005;64(2):128–33.
15. Atlas SW, Lavi E, Fisher PG. Intra-axial brain tumors. In: Atlas SW, editor. *Magnetic resonance imaging of the brain and spine*. 3rd edition. Philadelphia: Lippincott Williams Wilkins; 2002.

16. Forsyth PA, Petrov E, Mahallati H, et al. Prospective study of postoperative magnetic resonance imaging in patients with malignant gliomas. *J Clin Oncol* 1997;15(5):2076–81.
17. Vidiri A, Carapella CM, Pace A, et al. Early post-operative MRI: correlation with progression-free survival and overall survival time in malignant gliomas. *J Exp Clin Cancer Res* 2006;25(2):177–82.
18. Joffe P, Thomsen HS, Meusel M. Pharmacokinetics of gadodiamide injection in patients with severe renal insufficiency and patients undergoing hemodialysis or continuous ambulatory peritoneal dialysis. *Acad Radiol* 1998;5:491–502.
19. Wiginton CD, Kelly B, Oto A, et al. Gadolinium-based contrast exposure, nephrogenic systemic fibrosis, and gadolinium detection in tissue. *AJR Am J Roentgenol* 2008;190(4):1060–8.
20. Cowper SE. Nephrogenic systemic fibrosis: an overview. *J Am Coll Radiol* 2008;5(1):23–8.
21. Louis DN, Ohgaki H, Wiestler OD, et al. The 2007 WHO classification of tumours of the central nervous system. *Acta Neuropathol* 2007;114(2):97–109.
22. Koeller KK, Rushing EJ. From the archives of the AFIP: pilocytic astrocytoma: radiologic-pathologic correlation. *Radiographics* 2004;24(6):1693–708.
23. Beni-Adani L, Gomori M, Spektor S, et al. Cyst wall enhancement in pilocytic astrocytoma: neoplastic or reactive phenomenon. *Pediatr Neurosurg* 2000;32:234–9.
24. Arai K, Sato N, Aoki J, et al. MR signal of the solid portion of pilocytic astrocytoma on T2-weighted images: is it useful for differentiation from medulloblastoma? *Neuroradiology* 2006;48(4):233–7.
25. Lipper MH, Eberhard DA, Phillips CD, et al. Pleomorphic xanthoastrocytoma, a distinctive astroglial tumor: neuroradiologic and pathologic features. *AJNR: Am J Neuroradiol* 1993;14:1397–404.
26. Crespo-Rodriguez AM, Smirniotopoulos JG, Rushing EJ. MR and CT imaging of 24 pleomorphic xanthoastrocytomas (PXA) and a review of the literature. *Neuroradiology* 2007;49(4):307–15.
27. Luat AF, Makki M, Chugani HT. Neuroimaging in tuberous sclerosis complex. *Curr Opin Neurol* 2007;20(2):142–50.
28. Nishio S, Morioka T, Suzuki S, et al. Subependymal giant cell astrocytoma: clinical and neuroimaging features of four cases. *J Clin Neurosci* 2001;8(1):31–4.
29. Wessels PH, Weber WE, Raven G, et al. Supratentorial grade II astrocytoma: biological features and clinical course. *Lancet Neurol* 2003;2(7):395–403.
30. Recht LD, Bernstein M. Low-grade gliomas. *Neurol Clin* 1995;13:847–59.
31. Barker FG 2nd, Chang SM, Huhn SL, et al. Age and the risk of anaplasia in magnetic resonance-nonenhancing supratentorial cerebral tumors. *Cancer* 1997;80(5):936–41.
32. See SJ, Gilbert MR. Anaplastic astrocytoma: diagnosis, prognosis, and management. *Semin Oncol* 2004;31(5):618–34.
33. Tortosa A, Vinolas N, Villa S, et al. Prognostic implication of clinical, radiologic, and pathologic features in patients with anaplastic gliomas. *Cancer* 2003;97(4):1063–71.
34. Peretti-Viton P, Brunel H, Chinot O, et al. Histological and MR correlations in gliomatosis cerebri. *J Neurooncol* 2002;59(3):249–59.
35. Vates GE, Chang S, Lamborn KR, et al. Gliomatosis cerebri: a review of 22 cases. *Neurosurgery* 2003;53(2):261–71.

36. Osborn AG. Diagnostic imaging: brain. 1st edition. Salt Lake City: Amirsys; 2004.
37. Pierallini A, Bonamini M, Pantano P, et al. Radiological assessment of necrosis in glioblastoma: variability and prognostic value. *Neuroradiology* 1998;40(3):150–3.
38. Lafitte F, Morel-Precetti S, Martin-Duverneuil N, et al. Multiple glioblastomas: CT and MR features. *Eur Radiol* 2001;11(1):131–6.
39. Heimberger AB, Hlatky R, Suki D, et al. Prognostic effect of epidermal growth factor receptor and EGFR vIII in glioblastoma multiforme patients. *Clin Cancer Res* 2005;11:1462–6.
40. Lacroix M, Abi-Said D, Fourney DR, et al. A multivariate analysis of 416 patients with glioblastoma multiforme: prognosis, extent of resection, and survival. *J Neurosurg* 2001;95(2):190–8.
41. White ML, Zhang Y, Kirby P, et al. Can tumor contrast enhancement be used as a criterion for differentiating tumor grades of oligodendrogliomas? *AJNR: Am J Neuroradiol* 2005;26(4):784–90.
42. Jenkinson MD, du Plessis DG, Smith TS, et al. Histological growth patterns and genotype in oligodendroglial tumours: correlation with MRI features. *Brain* 2006;129:1884–91.
43. Megyesi JF, Kachur E, Lee DH, et al. Imaging correlates of molecular signatures in oligodendrogliomas. *Clin Cancer Res* 2004;10(13):4303–6.
44. Daumas-Duport C, Varlet P, Tucker ML, et al. Oligodendrogliomas. Part I: patterns of growth, histological diagnosis, clinical and imaging correlations: a study of 153 cases. *J Neurooncol* 1997;34:37–59.
45. Reiche W, Grunwald I, Hermann K, et al. Oligodendrogliomas. *Acta Radiol* 2002;43(5):474–82.
46. Mermuys K, Jeuris W, Vanhoenacker PK, et al. Best cases from the AFIP: supratentorial ependymoma. *Radiographics* 2005;25(2):486–90.
47. Comi AM, Backstrom JW, Burger PC, et al. Clinical and neuroradiologic findings in infants with intracranial ependymomas. *Pediatric Oncology Group. Pediatr Neurol* 1998;18(1):23–9.
48. Bühring U, Herrlinger U, Krings T, et al. MRI features of primary central nervous system lymphomas (PCNSL) at presentation. *Neurology* 2001;57:393–6.
49. Kuker W, Nagele T, Korfel A, et al. Primary central nervous system lymphomas (PCNSL): MRI features at presentation in 100 patients. *J Neurooncol* 2005;72:169–77.
50. Mohile NA, Abrey LE. Primary central nervous system lymphoma. *Neurol Clin* 2007;25(4):1193–207.
51. Slone HW, Blake JJ, Shah R, et al. CT and MRI findings of intracranial lymphoma. *AJR: Am J Roentgenol* 2005;184(5):1679–85.
52. Bendszus M, Warmuth-Metz M, Klein R, et al. Sequential MRI and MR spectroscopy in embolized meningiomas: correlation with surgical and histopathological findings. *Neuroradiology* 2002;44(1):77–82.
53. Tamiya T, Ono Y, Matsumoto K, et al. Peritumoral brain edema in intracranial meningiomas: effects of radiological and histological factors. *Neurosurgery* 2001;49(5):1046–51 [discussion 1051–2].
54. Maiuri F, Iaconetta G, de Divitiis O, et al. Intracranial meningiomas: correlations between MR imaging and histology. *Eur J Radiol* 1999;31(1):69–75.
55. Chenevert TL, Sundgren PC, Ross BD. Diffusion imaging: insight to cell status and cytoarchitecture. *Neuroimaging Clin N Am* 2006;16(4):619–32.

56. Chen S, Ikawa F, Kurisu K, et al. Quantitative MR evaluation of intracranial epidermoid tumors by fast fluid-attenuated inversion recovery imaging and echo-planar diffusion-weighted imaging. *AJNR: Am J Neuroradiol* 2001;22(6):1089–96.
57. Hartmann M, Jansen O, Heiland S, et al. Restricted diffusion within ring enhancement is not pathognomonic for brain abscess. *AJNR: Am J Neuroradiol* 2001;22(9):1738–42.
58. Kono K, Inoue Y, Nakayama K, et al. The role of diffusion-weighted imaging in patients with brain tumors. *AJNR: Am J Neuroradiol* 2001;22:1081–8.
59. Filippi CG, Edgar MA, Ulug AM, et al. Appearance of meningiomas on diffusion-weighted images: correlating diffusion constants with histopathologic findings. *AJNR: Am J Neuroradiol* 2001;22:65–72.
60. Murakami R, Sugahara T, Nakamura H, et al. Malignant supratentorial astrocytoma treated with postoperative radiation therapy: prognostic value of pretreatment quantitative diffusion-weighted MR imaging. *Radiology* 2007;243:493–9.
61. Lu S, Ahn D, Johnson G, et al. Peritumoral diffusion tensor imaging of high-grade gliomas and metastatic brain tumors. *AJNR* 2003;24:937–41.
62. Yamasaki F, Kurisu K, Satoh K, et al. Apparent diffusion coefficient of human brain tumors of MR imaging. *Radiology* 2005;235:985–91.
63. Provenzale JM, McGraw P, Mhatre P, et al. Peritumoral brain regions in gliomas and meningiomas: investigation with isotropic diffusion-weighted MR imaging and diffusion-tensor MR imaging. *Radiology* 2004;232(2):451–60.
64. Smith JS, Cha S, Mayo MC, et al. Serial diffusion-weighted magnetic resonance imaging in cases of glioma: distinguishing tumor recurrence from postresection injury. *J Neurosurg* 2005;103:428–38.
65. Cha S. Update on brain tumor imaging: from anatomy to physiology. *AJNR: Am J Neuroradiol* 2006;27:475–87.
66. Asao C, Korogi Y, Kitajima M, et al. Diffusion-weighted imaging of radiation-induced brain injury for differentiation from tumor recurrence. *AJNR: Am J Neuroradiol* 2005;26:1455–60.
67. Yu CS, Li KC, Xuan Y, et al. Diffusion tensor tractography in patients with cerebral tumors: a helpful technique for neurosurgical planning and postoperative assessment. *Eur J Radiol* 2005;56:197–204.
68. Jena R, Price SJ, Baker C, et al. Diffusion tensor imaging: possible implications for radiotherapy treatment planning of patients with high-grade glioma. *Clin Oncol* 2005;17:581–90.
69. Toh CH, Wong AMC, Wei KC, et al. Peritumoral edema of meningiomas and metastatic brain tumors: differences in diffusion characteristics evaluated with diffusion-tensor MR imaging. *Neuroradiology* 2007;49:489–94.
70. Price SJ, Jena R, Burnet NG, et al. Improved delineation of glioma margins and regions of infiltration with the use of diffusion tensor imaging: an image-guided biopsy study. *AJNR: Am J Neuroradiol* 2006;27:1969–74.
71. Price SJ, Pena A, Burnet NG, et al. Detecting glioma invasion of the corpus callosum using diffusion tensor imaging. *Br J Neurosurg* 2004;18:391–5.
72. Cha S. CNS tumors: monitoring therapeutic response and outcome prediction. *Top Magn Reson Imaging* 2006;17:63–8.
73. Fan GG, Deng QL, Wu ZH, et al. Usefulness of diffusion/perfusion-weighted MRI in patients with nonenhancing supratentorial brain gliomas: a valuable tool to predict tumour grading. *Br J Radiol* 2006;79:652–8.

74. Cha S, Tihan T, Crawford F, et al. Differentiation of low grade oligodendrogliomas from low-grade astrocytomas by using quantitative blood-volume measurements derived from dynamic susceptibility contrast-enhanced MR imaging. *AJNR: Am J Neuroradiol* 2005;26:266–73.
75. Law M, Oh S, Babb JS, et al. Low-grade gliomas: dynamic susceptibility-weighted contrast-enhanced perfusion MR imaging: prediction of patient clinical response. *Radiology* 2006;238:658–67.
76. Weber MA, Zoubaa S, Schlieter M, et al. Diagnostic performance of spectroscopic and perfusion MRI for distinction of brain tumors. *Neurology* 2006;66:1899–906.
77. Law M, Cha S, Knopp EA, et al. High grade gliomas and solitary metastases: differentiation by using perfusion and proton spectroscopic MR imaging. *Radiology* 2002;222:715–21.
78. Maia AC Jr, Malheiros SM, da Rocha AJ, et al. MR cerebral blood volume maps correlated with vascular endothelial growth factor expression and tumor grade in nonenhancing gliomas. *AJNR: Am J Neuroradiol* 2005;26:777–83.
79. Warmuth C, Günther M, Zimmer C. Quantification of blood flow in brain tumors: comparison of arterial spin labeling and dynamic susceptibility-weighted contrast-enhanced MR imaging. *Radiology* 2003;228:523–32.
80. Essig M, Weber MA, Von Tengg-Kobligk H, et al. Contrast-enhanced magnetic resonance imaging of central nervous system tumors: agents, mechanisms, and applications. *Top Magn Reson Imaging* 2006;17:89–106.
81. Astrakas LG, Zurakowski D, Tzika AA, et al. Noninvasive magnetic resonance spectroscopic imaging biomarkers to predict the clinical grade of pediatric brain tumors. *Clin Cancer Res* 2004;10:8220–8.
82. Fountas KN, Kapsalaki EZ, Vogel RL, et al. Noninvasive histologic grading of solid astrocytomas using proton magnetic resonance spectroscopy. *Stereotact Funct Neurosurg* 2004;82:90–7.
83. Stadlbauer A, Gruber S, Nimski C, et al. Preoperative grading of gliomas using metabolite quantification with high-spatial-resolution proton MR spectroscopic imaging. *Radiology* 2006;238:958–69.
84. Tzika AA, Zarifi MK, Goumnerova L, et al. Neuroimaging in pediatric brain tumors: GD-DTPA-enhanced, hemodynamic, and diffusion MR imaging compared with MR spectroscopic imaging. *AJNR: Am J Neuroradiol* 2002;23:322–33.
85. Hollingworth W, Medina LS, Lenkinski RE, et al. A systematic literature review of magnetic resonance spectroscopy for the characterization of brain tumors. *AJNR: Am J Neuroradiol* 2006;27:1404–11.
86. Sibtain NA, Howe FA, Saunders DE. The clinical value of proton magnetic resonance spectroscopy in adult brain tumors. *Clin Radiol* 2007;62:109–19.
87. Henson JW, Ulmer S, Harris GJ. Brain tumor imaging in clinical trials. *AJNR: Am J Neuroradiol* 2008;29(3):419–24.
88. Therasse P, Arbuck SG, Eisenhauer EA, et al. New guidelines to evaluate the response to treatment in solid tumors: European Organization for Research and Treatment of Cancer, National Cancer Institute of the United States, National Cancer Institute of Canada. *J Natl Cancer Inst* 2000;92:205–16.
89. Macdonald DR, Cascino TL, Schold SC, et al. Response criteria for phase II studies of malignant glioma. *J Clin Oncol* 1990;8:1277–80.
90. Galanis E, Buckner JC, Maurer MJ, et al. Validation of neuroradiologic response assessment in gliomas: measurement by RECIST, two-dimensional, computer-assisted tumor area, and computer-assisted tumor volume methods. *Neuro Oncol* 2006;8:156–65.

91. Ulmer S, Braga TA, Barker FG, et al. Clinical and radiographic features of peritumoral infarction following resection of glioblastoma. *Neurology* 2006;67:1668–70.
92. Pope WB, Lai A, Nghiemphu P, et al. MRI in patients with high-grade gliomas treated with bevacizumab and chemotherapy. *Neurology* 2006;66:1258–60.
93. Bogomolny DL, Petrovich NM, Hou BL, et al. Functional MRI in the brain tumor patient. *Top Magn Reson Imaging* 2004;15(5):325–35.
94. Medina LS, Aguirre E, Bernal B, et al. Functional MRI imaging versus WADA test for evaluation of language lateralization: cost analysis. *Radiology* 2004;230:49–54.
95. Haberg A, Kvistad KA, Unsgard G, et al. Preoperative blood oxygen level-dependent functional magnetic resonance imaging in patients with primary brain tumors: clinical application and outcome. *Neurosurgery* 2004;54:902–14.
96. Sunaert S. Presurgical planning for tumor resectioning. *J Magn Reson Imaging* 2006;23(6):887–905.
97. Petrella JR, Shah LM, Harris KM, et al. Preoperative functional MR imaging localization of language and motor areas: effect on therapeutic decision making in patients with potentially resectable brain tumors. *Radiology* 2006;240:793–802.
98. Yuh WT, Christoforidis GA, Koch RM, et al. Clinical magnetic resonance imaging of brain tumors at ultrahigh field: a state-of-the-art review. *Top Magn Reson Imaging* 2006;17:53–61.
99. Lupo JM, Lee MC, Han ET, et al. Feasibility of dynamic susceptibility contrast perfusion MR imaging at 3 T using a standard quadrature head coil and eight-channel phased-array coil with and without SENSE reconstruction. *J Magn Reson Imaging* 2006;24:520–9.
100. Roberts TP, Mikulis D. Neuro MR: principles. *J Magn Reson Imaging* 2007;26(4):823–37.
101. Krautmacher C, Willinek WA, Tschampa HJ, et al. Brain tumors: full- and half-dose contrast-enhanced MR imaging at 3.0 T compared with 1.5 T: initial experience. *Radiology* 2005;237:1014–9.
102. Sehgal V, Delproposto Z, Haddar D, et al. Susceptibility-weighted imaging to visualize blood products and improve tumor contrast in the study of brain masses. *J Magn Reson Imaging* 2006;24(1):41–51.
103. Jolesz FA, Talos IF, Warfield SK, et al. Magnetic resonance image-guided neurosurgery. In: Newton HB, Jolesz FA, editors. *Handbook of neuro-oncology neuroimaging*. 1st edition. New York: Elsevier; 2008. p. 171–80.
104. Chu RM, Tummala RP, Hall WA. Intraoperative magnetic resonance image-guided neurosurgery. *Neurosurg Q* 2003;13:234–50.
105. Hall WA, Truwit CL. Intraoperative MR-guided neurosurgery. *J Magn Reson Imaging* 2008;27(2):368–75.
106. Busse H, Schmitgen A, Trantakis C, et al. Advanced approach for intraoperative MRI guidance and potential benefit for neurosurgical applications. *J Magn Reson Imaging* 2006;24(1):140–51.
107. Hall WA, Galicich W, Bergman T, et al. 3-Tesla intraoperative MRI imaging for neurosurgery. *J Neurooncol* 2006;77:297–303.
108. Kinoshita M, McDannold N, Jolesz FA, et al. Targeted delivery of antibodies through the blood-brain barrier by MRI-guided focused ultrasound. *Biochem Biophys Res Commun* 2006;340(4):1085–90.
109. Hynynen K, McDannold N, Sheikov NA, et al. Local and reversible blood-brain barrier disruption by noninvasive focused ultrasound at frequencies suitable for trans-skull sonications. *Neuroimage* 2005;24(1):12–20.

110. Anderson SA, Glod J, Arbab AS, et al. Non-invasive MR imaging of magnetically labeled stem cells to directly identify neovasculature in a glioma model. *Blood* 2005;105:420–5.
111. Hsu AR, Chen X. Advances in anatomic, functional, and molecular imaging of angiogenesis. *J Nucl Med* 2008;49:511–4.
112. Shah K, Jacobs A, Breakefield XO, et al. Molecular imaging of gene therapy for cancer. *Gene Ther* 2004;11:1175–87.
113. Jackson A, O'Connor JPB, Parker GJM, et al. Imaging tumor vascular heterogeneity and angiogenesis using DCE-MRI. *CCR focus. Clin Cancer Res* 2007;13:3449–59.

ASN Scottsdale, AZ 2015

Brain Tumor Syllabus

*Laszlo L. Mechtler, M.D, FAAN
Medical Director, DENT Neuro-Oncology Center
Chief of Neuro-Oncology
Roswell Park Cancer Institute
Neuroimager*

ASTROCYTOMA

Terminology

- Primary brain tumor of astrocytic origin with intrinsic tendency for malignant progression, degeneration into anaplastic astrocytoma (AA).

Imaging Findings

- Best diagnostic clue: Focal or diffuse nonenhancing white matter (WM) mass
- Cerebral hemispheres, supratentorial 2/3
- May appear circumscribed on imaging but isn't; tumor cells typically found beyond imaged signal abnormality!

Top Differential Diagnoses

- Anaplastic astrocytoma (AA)
- Ischemia
- Cerebritis

- Oligodendroglioma
- Herpes encephalitis
- Status epilepticus

Pathology

- Represents 25-30% of gliomas in adults
- 10-15% of all astrocytomas
- Diffusely infiltrating mass with blurring of GM/WM interface
- WHO grade II

Clinical Issues

- Majority occur between ages of 20-45 years
- Inherent tendency for malignant progression of AA = major cause of mortality
- Median survival 6-10 years.



PEDIATRIC BRAINSTEM GLIOMA

Terminology

- Tectal glioma (tectal)

- Focal tegmental mesencephalic (FTM)
- Diffuse (intrinsic) pontine glioma (DPG)
- Heterogeneous group of focal or diffuse gliomas involving mesencephalon, pons, or medulla

Imaging Findings

- Classic imaging appearance varies with tumor type and location
- Tectal: Pilocytic, focal, variable enhancement/Ca ++
- FTM: Pilocytic, cyst plus nodule
- DPG: Fibrillary, diffuse, nonenhancing
- All BSG are not equal! Geography predict prognosis
- Borders/margins predictive of prognosis

Top Differential Diagnoses

- Congenital aqueductal stenosis vs tectal glioma
- Alexander disease vs tectal glioma
- Neurofibromatosis type 1 vs DPG
- Other brainstem gliomas

Pathology

- General path comments: No metastases outside CNS
- Epidemiology: 10-20% pediatric brain tumors

Diagnostic Checklist

- Not all expansile brainstem lesions are neoplasms
- Geography predicts prognosis
-

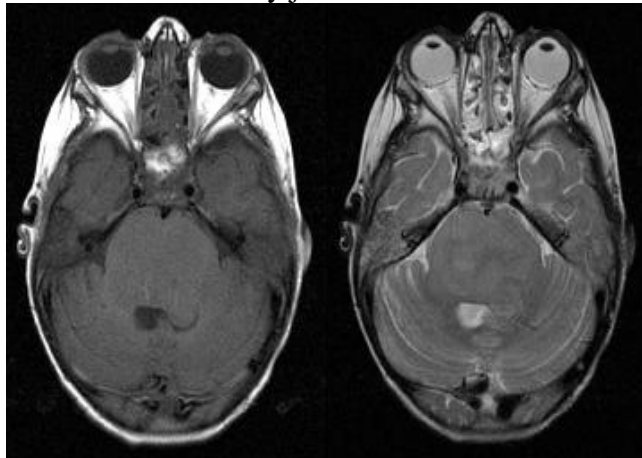
PEARLS IN THE DIAGNOSIS OF BRAIN STEM GLIOMAS

- Peak age: 6-8 years
- Signal: Hyperintense on T2 (95%), exophytic tumor produces brighter signal
- Growth patterns
 - a. Cystic tectum (20%)

- b. Infiltrative, pons (70%)
- Dedifferentiation of glioblastoma multiforme 5-7% of pediatric cases
- Location
 - a. Pontomedullary (80%)
 - b. Midbrain (60%)
 - c. Cerebellum (40%)
 - d. Cervical cord (35%)
 - e. Posterior thalamus (30%)
- Enhancement: Variable and may not be present
- Calcification: Less than 4%
- Differential diagnosis
 - a. Vascular malformation (flow void or hemorrhage signal, non-expansile)
 - b. Metastases (adults with history of primary neoplasm, contrast enhancement)

RANGE OF NORMAL ANTEROPOSTERIOR BRAIN STEM DIAMETERS

- Midbrain tegmentum: 11-15 mm
- Pons: 24-29 mm
- Pontomedullary junction: 14-17 mm
- Cervicomedullary junction: 8-11 mm



ANAPLASTIC ASTROCYTOMA

Terminology

- Diffusely infiltrating astrocytoma with focal or diffuse anaplasia and a marked proliferative potential

Imaging Findings

- Infiltrating mass that predominately involves white matter (WM)
- Variable enhancement, typically none; may be focal or patchy
- Hemispheric WM, frontal & temporal lobes common
- Neoplastic cells almost always found beyond areas of abnormal signal intensity

Top Differential Diagnoses

- Low grade glioma
- Glioblastoma multiforme (GBM)
- Cerebritis
- Ischemia
- Oligodendroglioma
- Status epilepticus
- Herpes encephalitis

Pathology

- AA have histologic and imaging characteristics among spectrum between low grade astrocytoma and GMB
- 1/3 of astrocytomas
- May appear discrete but tumor always infiltrates adjacent brain
- WHO grade III

Clinical Issues

- Median survival 2-3 years
- Commonly arise as recurrence after resection of a grade II tumor

GLIOBLASTOMA MULTIFORME

Terminology

- Rapidly enlarging malignant astrocytic tumor characterized by necrosis and neovascularity
- Most common of all primary intracranial neoplasms

Imaging Findings

- Best diagnostic clue: Thick, irregular-enhancing rind of neoplastic tissue surrounding necrotic core

Top Differential Diagnoses

- Abscess
- Metastasis
- Primary CNS lymphoma
- Anaplastic astrocytoma (AA)
- “Tumefactive” demyelination
- Subacute ischemia
- Status epilepticus

Pathology

- Two types, primary (de novo) and secondary (degeneration from lower grade astrocytoma)
- 50-60% of astrocytomas
- WHO grade IV

Clinical Issues(Filippi et al., 1996)

- Age: Peak 45-70 years but may occur at any age
- Relentless progression
- Prognosis is dismal (death in 9-12 months)

Diagnostic Checklist

- Viable tumor extends far beyond signal abnormalities!

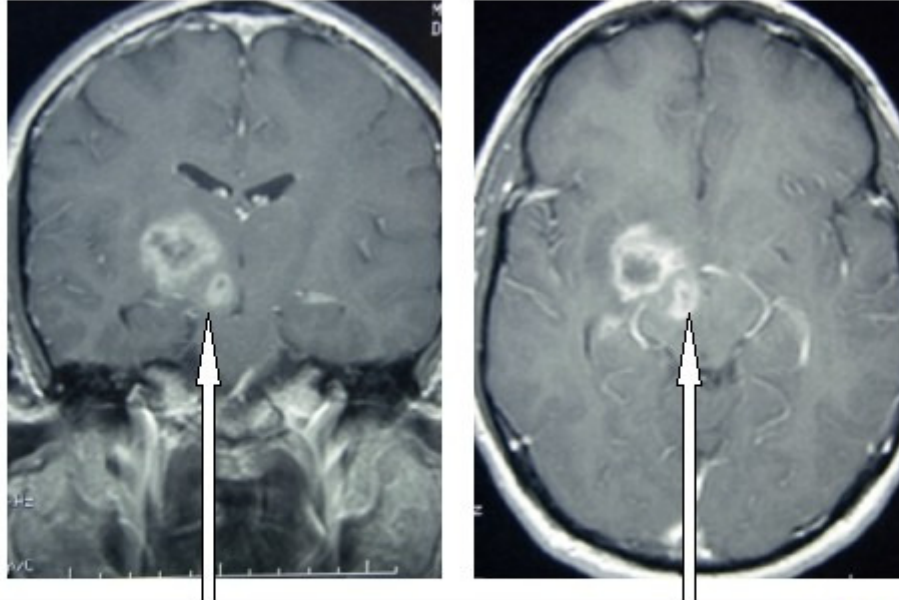


Figure 1A (Left): MRI Scan (Coronal View-Gadolinium enhanced). 45 year old male with a deep seated Right Thalamic region Glioblastoma with direct infiltration of the Brainstem (Arrow).

Figure 1B (Right): MRI Scan (Transaxial View-Gadolinium enhanced) in the same patient as Figures 1A & 2.) Partially Cystic Right Thalamic Region Glioblastoma infiltrates the Brainstem along fibre tracts (Arrow).

GLIOSARCOMA

Terminology

- Rare malignant neoplasm with both glial, mesenchymal elements

Imaging Findings

- Heterogeneously enhancing mass with dural invasion, +/- skull involvement

May be indistinguishable from GBM

Top Differential Diagnoses

- Glioblastoma multiforme (GBM)
- Metastasis
- Abscess
- Hemangiopericytoma
- Malignant meningioma

Clinical Issues

- Poor prognosis, median survival of 6-12 months

GLIOMATOSIS CEREBRI

Terminology

- Diffusely infiltrating glial tumor involving two or more lobes, frequently bilateral
- Infiltrative extent of tumor is out of proportion to histologic and clinical features

Imaging Findings

- Best diagnostic clue: T2 hyperintense infiltrating mass with enlargement of involved structures
- Typically hemispheric white matter involvement, may also involve cortex (19%)
- May cross corpus callosum or massa intermedia
- Morphology: Infiltrates, enlarges yet preserves underlying brain architecture
- Typically no or minimal enhancement
- Marked elevation of myo-inositol (mI)

Top Differential Diagnoses

- Arteriosclerosis
- Anaplastic astrocytoma (AA)
- Viral encephalitis

- Lymphoma

Pathology

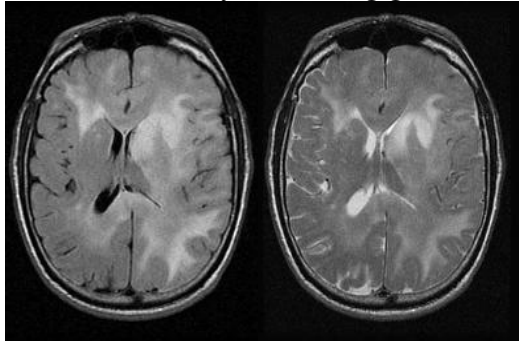
- Underlying brain architecture preserved
- Usually WHO grade III

Clinical Issues

- Peak incidence between 40-50 years
- Poor prognosis

Diagnostic Checklist

- Rare diffusely infiltrating glial tumor that can be mistaken for nonneoplastic WM disease



PILOCYTIC ASTROCYTOMA

Terminology

- Pilocytic astrocytoma (PA), juvenile pilocytic astrocytoma (JPA)

Imaging Findings

- Cystic cerebellar mass with enhancing mural nodule
- Enlarged optic nerve/chiasm/tract with variable enhancement
- Paradoxical findings: MRS does not accurately reflect historical behavior of tumor
- Multiplanar or 3D volume post contrast imaging key to showing point to origin and degree of extension

Top differential Diagnoses

- Medulloblastoma (PNET-MB)
- Pilomyxoid astrocytoma

Pathology

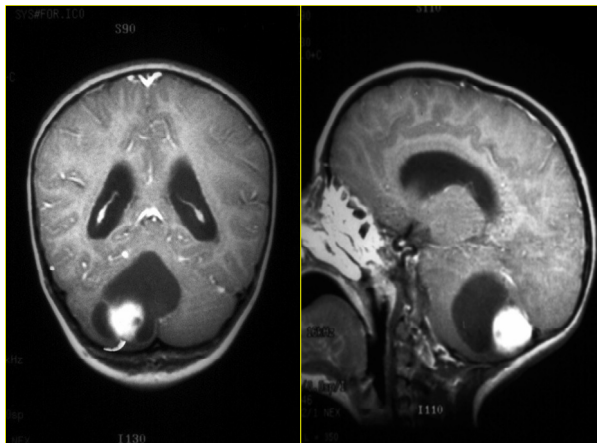
- 15% of NF1 patients develop PAs, most commonly in optic pathway
- Up to 1/3 of patients with optic pathway PAs have NF1
- WHO grade 1

Clinical Issues

- Peak incidence: 5-15 years of age
- Older than children with medulloblastoma

Diagnostic Checklist

- Generally not a reasonable diagnostic consideration in adults
- An enhancing intra-axial tumor with cystic change in a “middle-age” child is more likely to be PA than anything else



PLEOMORPHIC XANTHOASTROCYTOMA

Terminology

- Distinct type of (usually) benign supratentorial astrocytoma found almost exclusively in young adults

Imaging Findings

- Supratentorial cortical mass with adjacent enhancing dural “tail”
- Temporal lobe most common



Top Differential Diagnoses

- Ganglioglioma
- Pilocytic astrocytoma
- Dysembryoplastic neuroepithelial tumor (DNET)

- Oligodendroglioma
- Meningioma
- Low grade astrocytoma (Grade II)

Pathology

- Superficial, circumscribed astrocytic tumor noted for cellular pleomorphism and xanthomatous change
- < 1% of all astrocytomas
- Cystic mass with mural nodule abutting meninges
- Deep margin may show infiltration of parenchyma
- WHO grade II

Clinical Issues

- Majority with long-standing epilepsy, often partial complex seizures (temporal lobe)
- Tumor of children/young adults

Diagnostic Checklist

- Cortical mass & meningeal thickening in a young adult with long seizure history? Think PXA!

SUBPENDYMAL GIANT CELL ASTROCYTOMA

Imaging Findings

- Enlarging, enhancing intraventricular mass in patient with tuberous sclerosis complex (TSC)
- Location: Almost always near foramen of Monro
- Well marginated, often lobulated
- Heterogeneous, strong enhancement
- Presence of interval growth suggests SGCT
- Enhancement alone does not allow discrimination from hamartoma
- FLAIR MR to detect subtle CNS features of TSC
- Recommend brain MR with contrast every 1-2 years for SGCT follow-up

Top Differential Diagnoses

- Choroid plexus tumors
- Astrocytoma
- Germinoma
- Subependymoma

Pathology

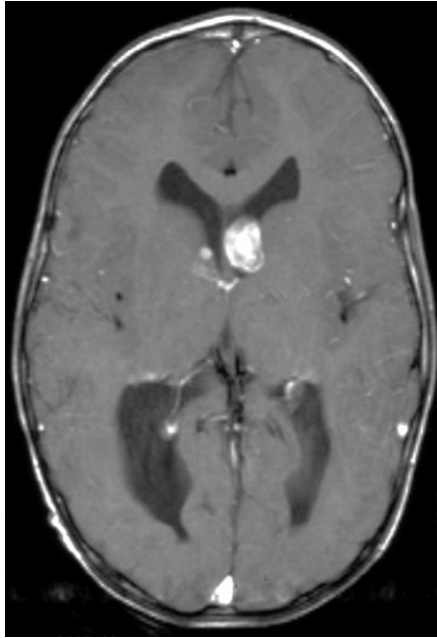
- Most common CNS neoplasm in TSC
- Does not seed CSF pathways
- WHO grade I

Clinical Issues

- Increased ICP secondary to tumor obstructing foramen of Monro

Diagnostic Checklist

- SGCA in tuberous sclerosis patient with worsening seizures and/or symptoms of ventricular obstruction



OLIGODENDROGLIOMA

Terminology

- Well-differentiated, slowly growing but diffusely infiltrating cortical/subcortical tumor

Imaging Findings

- Best diagnostic clue: Partially Ca⁺⁺ subcortical/cortical mass in middle-aged adult
- Typically involves subcortical white matter (WM) and cortex
- Majority supratentorial (85%), hemispheric WM
- Most common site is frontal lobe
- May involve temporal, parietal or occipital lobes
- Morphology: Infiltrative mass that appears well demarcated
- Majority calcify, nodular or clumped Ca⁺⁺ (70-90%)

Top Differential Diagnoses

- Anaplastic oligodendroglioma (AO)
- Astrocytoma
- Ganglioglioma
- Dysembryoplastic neuroepithelial tumor (DNET)
- Pleomorphic xanthoastrocytoma (PXA)
- Cerebritis
- Ischemia

Pathology

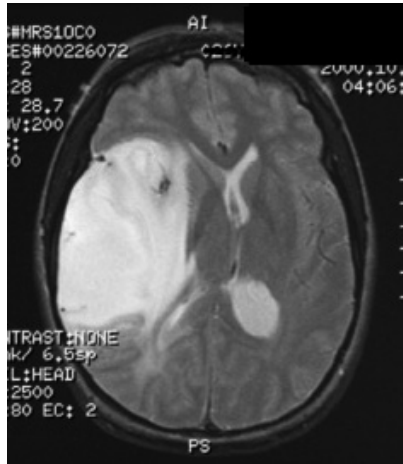
- WHO grade II

Clinical Issues

- Seizures, headaches
- Peak incidence 4th and 5th decades
- Surgical resection in primary treatment

Pearls in the Diagnosis of Oligodendroglioma

- Peak age: 30-50 years
- Calcification: 80%
- Cyst formation: 10%
- Edema: 50%
- Location: frontotemporal centrum
- Hemorrhage: 80-90%
- Margins: poorly defined; therefore, all areas of T2 relaxation prolongation should be radiated
- Enhancement: moderate and inhomogeneous
- Differential Diagnosis:
 - Meningioma (pseudocapsule, extra-axial)
 - Ganglioglioma (males, temporal lobe and anterior third ventricle predilection)
 - Calcified glioma (less infiltrative, more mass effect, less calcification)
 - Arteriovenous malformation (hypointense flow void signal, T2 dependent hemosiderin)



ANAPLASTIC OLIGODENDROGLIOMA

Terminology

- Oligodendroglioma with focal or diffuse histologic features of malignancy

Imaging Findings

- Best diagnostic clue: Calcified frontal lobe mass involving cortex/subcortical white matter (WM)
- May appear discrete, but always infiltrative
- Neoplastic cells almost always found beyond areas of abnormal signal intensity

Top Differential Diagnoses

- Oligodendroglioma
- Anaplastic multiforme (GBM)
- Cerebritis
- Ischemia

Pathology

- Well-differentiated (grade II) and anaplastic (grade III) types of oligodendroglioma
- Oligoastrocytoma (mixed tumor with 2 distinct neoplastic cell types) are common (50%)
- Oligos have better prognosis than astrocytomas of same grade
- Average number of chromosomes involved is higher in grade III than grade II oligos
- 20-50% of oligodendrogliomas are anaplastic
- WHO grade III

Clinical Issues

- Peak incidence fourth through sixth decade
- Median survival 4 years
- Local tumor recurrence common

EPENDYMOMA

Terminology

- Slow-growing tumor of ependymal cells

Imaging Findings

- Soft or “plastic” tumor: Squeezes out through 4th ventricle foramina into cisterns
- 2/3rd infratentorial, 4th ventricle
- 1/3rd supratentorial, majority periventricular WM
- Ca++ common (50%); +/- cysts, hemorrhage
- MR spectroscopy alone does not reliably differentiate ependymoma from astrocytoma or PNET-MB
- High-quality sagittal imaging can distinguish point of origin as floor vs roof of 4th ventricle

Top Differential Diagnoses

- Medulloblastoma (PNET-MB)

Pathology

- Arise from ependymal cells or ependymal rests
- Third most common posterior fossa tumor in children (after PA and PNET-MB)
- WHO grade II (low grade, well-differentiated)
- WHO grade III (high grade, anaplastic)

Clinical Issues

- Clinical profile: 1-5 yo with headache, vomiting
- Gross total resection + XRT correlates with improved survival

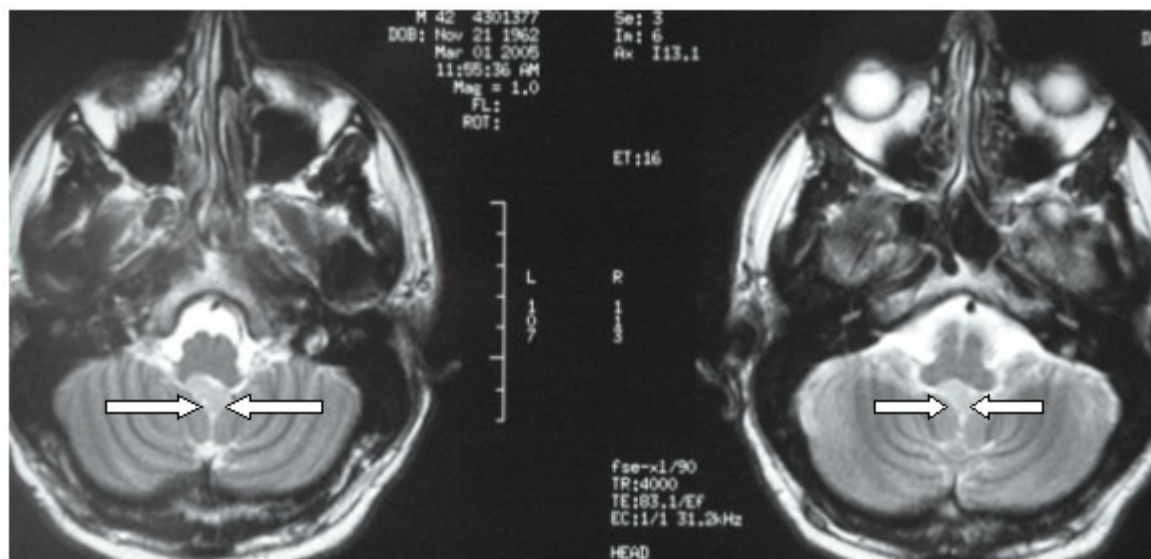
Diagnostic Checklist

- Indistinct interface with floor of 4th ventricle = ependymoma

Pearls in the Diagnosis of Ependymoma

- Tendency to involve the filum
- Hemorrhagic in a significant percentage of the cases, especially the myxopapillary form of the filum
- Tendency to form cysts
 - a. Marginal cysts located at the tumor edge and easily amenable to syringotomy decompression
 - b. Central cysts which are located within the lesion and must be excised if they are to be treated
- Ependymomas tend to have hypointense T1 and hyperintense T2 signal and either show cyst formation or signal inhomogeneity
- Filum location is a strong tip-off to the diagnosis (these lesions tend to seed the CSF and may be a result of drop metastases)
- Enhancement is moderate to marked

- Indistinct interface with roof of 4th ventricle = PNET-MB



MRI Scan (Transaxial View-same patient as Figures 1, 4 & 5) 4th Ventricular Ependymoma. The tumor (centrally located lighter "grey" mass) fills the 4th Ventricle in these images (Arrows)

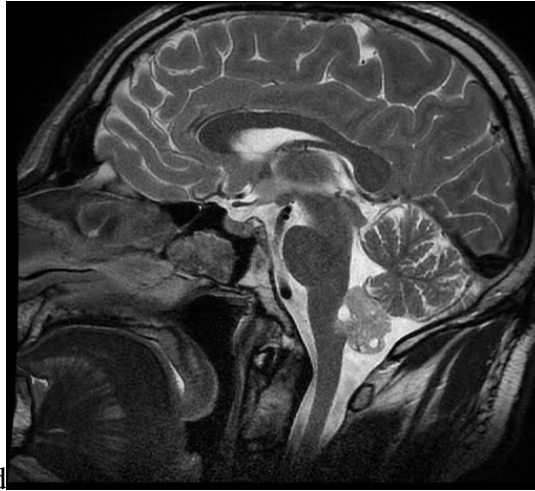
SUBEPENDYMOMA

Terminology

- Rare, benign well-differentiated intraventricular ependymal tumor

Imaging Findings

- Best diagnostic clue: T2 hyperintense lobular, nonenhancing intraventricular mass
- Intraventricular, inferior 4th ventricle typical (60%)
- Other: Lateral > 3rd ventricle > spinal cord
- Well-defined solid lobular mass
- When large, may see cysts, hemorrhage, Ca⁺⁺



- Variable enhancement, typically none to mild

Top Differential Diagnoses

- Ependymoma
- Central neurocytoma
- Subependymal giant cell astrocytoma
- Choroid plexus papilloma (CPP)
- Hemangioblastoma
- Metastases

Pathology

- WHO grade I

Clinical Issues

- Most asymptomatic
- Other signs/symptoms: Related to increased intracranial pressure, hydrocephalus
- Middle-aged/elderly adult, (typically 5th-6th decades)
- Surgical resection is curative in most cases

Diagnostic Checklist

- 4th or lateral ventricular hyperintense mass in an elderly male? Think sybependymoma!

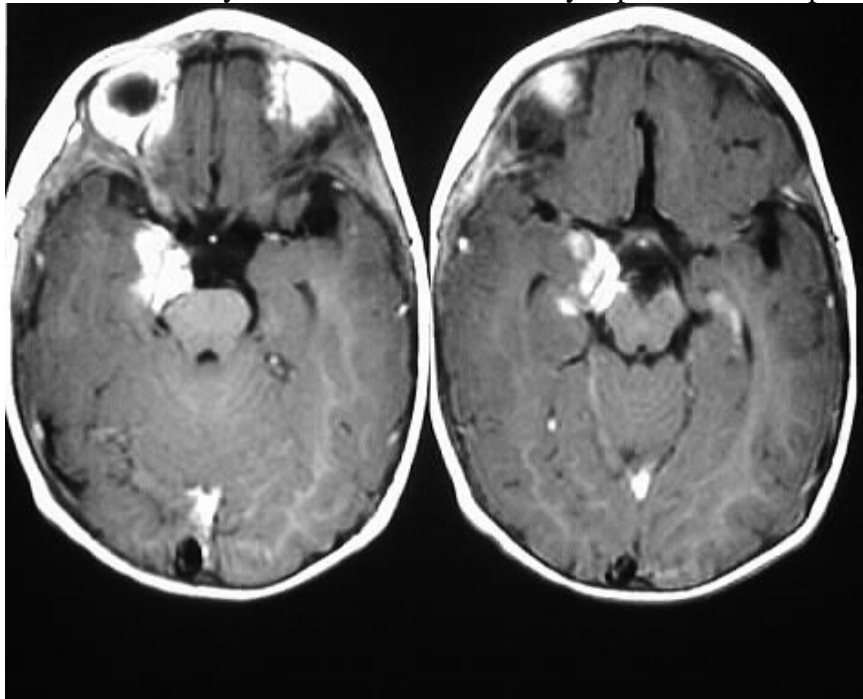
GANGLIOGLIOMA

Terminology

- Well differentiated, slowly growing neuroepithelial tumor composed of neoplastic ganglion cells and neoplastic glial cells

Imaging Findings

- Best diagnostic clue: Partially cystic, enhancing, cortically-based mass in child/young adult with TLE
- Can occur anywhere but most commonly superficial hemispheres, temporal lobe



Top Differential Diagnoses

- Pleomorphic xanthoastrocytoma (PXA)

- Dysembryoplastic neuroepithelial tumor (DNET)
- Pilocytic astrocytoma
- Low grade astrocytome (grade II)
- Oligodendroglioma

Pathology

- Cortical dysplasia is commonly associated
- Most common mixed neuronal-glial tumor
- WHO grade I and II

Clinical Issues

- Clinical profile: Most common neoplasm causing chronic temporal lobe epilepsy
- Excellent prognosis if surgical resection complete
- Malignant degeneration is rare, approximately 5-10% (glial component)

Diagnostic Checklist

- In young patient with history of temporal lobe epilepsy, think ganglioglioma
- Cyst with an enhancing mural nodule is classic, but nonspecific for ganglioglioma

Pearls in the Diagnosis of Ganglioglioma

- Age: 15-30 years
- Gender: slight male predominance
- Location: temporal lobe or anterosuperior third ventricle
- Signal: nonspecific hypointense T1 and hyperintense T2
- Enhancement: variable and nominal to moderate
- Cyst formation: 10%
- Hemorrhage: rare
- Calcification: 10-20%
- Insidious seizure history and lesion in the correct location are tipoffs to diagnosis
- Differential diagnosis:
 - Oligodendroglioma: more edema

- Vascular malformation: less mass effect, no edema, flow void, hemosiderin
- Colloid cyst: smaller size, hyperintense T1

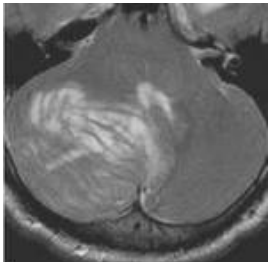
DYSPLASTIC CEREBELLAR GANGLIOCYTOMA

Terminology

- Best known as Lhermitte-Duclos disease (LDD)

Imaging Findings

- Best diagnostic clue: Widened cerebellar folia with striated appearance on MR
- Characteristics “layered” or striated” pattern of alternating isointense and hyperintense signal
- Also called “ laminated”, “corduroy”, “lamellar”, “folial”
- No diffusion disturbance on ADC maps
- T1 C+: Rare lesions enhance
- PET: Elevated 18-FDG uptake
- Elevated 201-thallium uptake on delayed imaging



Top Differential Diagnoses

- Cerebellar infarction
- Acute cerebellitis
- Leptomeningeal

Pathology

- Associated with Cowden syndrome
- Characterized by development of multiple hamartomas

- Increased risk of thyroid and breast carcinoma
- Some evidence supports that all cases of LDD have Cowden syndrome
- Replacement and expansion of granular layer by large neurons

Diagnostic Checklist

- Striated cerebellar hemisphere is “Aunt Minnie” for LDD

DESMOPLASTIC INFANTILE GANGLIOGLIOMA

Terminology

- Desmoplastic infantile (DIG, DIGG) or desmoplastic infantile astrocytoma (DIA)

Imaging Findings

- Large cyst + cortical-based enhancing tumor nodule
- Location: frontal > parietal > temporal
- Solid tumor module(s) enhance markedly
- Enhancement of leptomeninges, dura adjacent to solid tumor is typical

Top Differential Diagnosis

- Primitive neuroectodermal tumor (PNET)
- Supratentorial ependymoma
- Pleomorphic xanthoastrocytoma (PXA)
- Hemangioblastoma
- Ganglioglioma
- Pilocytic astrocytoma

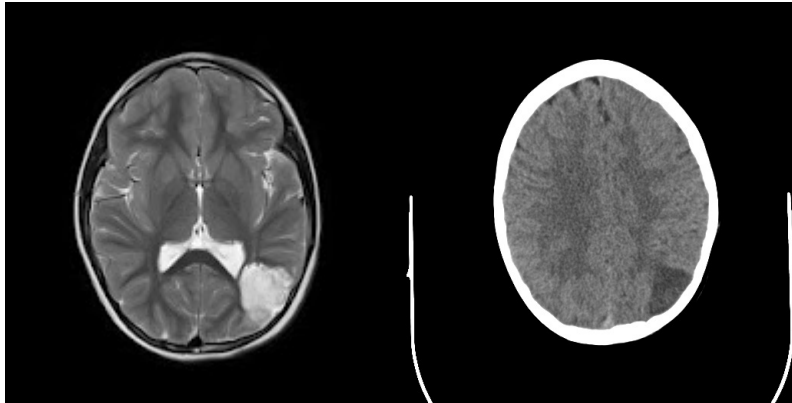
DNET

Terminology

- Dysembryoplastic neuroepithelial tumor (DNET)
- Benign, focal, intracortical mass superimposed on background of cortical dysplasia

Imaging Findings

- Best diagnostic clue: Well-demarcated, wedge-shaped “bubbly” intracortical mass in young patient with longstanding partial seizures
- Temporal lobe (often amygdale/hippocampus) most common site
- Intracortical mass scallops inner table of skull and “points” towards ventricle
- Minimal or no mass effect



Pathology

- Approximately 1-2% of primary brain tumors in patients < 20 years
- Reported in 5-80% of epilepsy specimens

Clinical Issues

- Clinical profile: Longstanding (difficult to control) partial complex seizures in child or young adult
- NO or very slow increase in size over time
- Rare recurrence
- Beware of atypical features (enhancement) on pre-op imaging

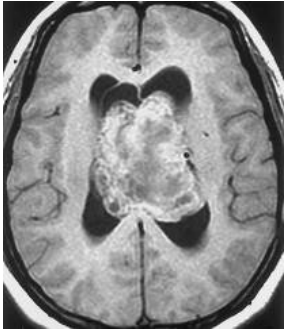
CENTRAL NEUROCYTOMA

Terminology

- Intraventricular neuroepithelial tumor with neuronal differentiation

Imaging Findings

- Best diagnostic clue: “Bubbly” mass in frontal horn or body of lateral ventricle
- Intraventricular mass attached to septum pellucidum
- Circumscribed, lobulated mass with intratumoral “cysts”
- Ca⁺⁺ common, 50-70%



Top Differential Diagnosis

- Subependymoma
- Subependymal giant cell astrocytoma (SGCA)
- Metastasis
- Ependymoma
- Choroid plexus papilloma (CPP)
- Meningioma
- Cavernous malformation

Pathology

- < 1% of all primary intracranial neoplasms
- Represents 50% of intraventricular tumors on patients 20-40 years
- Resembles oligodendroglioma
- WHO grade II

Clinical Issues

- Most common signs/symptoms: Headaches, increased intracranial pressure, mental status changes, seizure
- Hydrocephalus secondary to forearm of Monro obstruction
- Complete surgical resection is treatment of choice

PINEOBLASTOMA

Terminology

- Highly malignant, primitive embryonal tumor of pineal gland

Imaging Findings

- Large, heterogeneous pineal mass with “exploded”, peripheral Ca++
- Nearly 100% with obstructive hydrocephalus



Top Differential Diagnoses

- Germ cell tumors (GCTs)
- Meningioma
- Pineocytoma (PC)
- Metastases

Pathology

- PBs exhibit little to no differentiation, similar to other PNETs

Clinical Issues

- Elevated ICP (hydrocephalus): Headache, nausea, vomiting, lethargy, papilledema, abducens nerve palsy

Diagnostic Checklist

- Both PBs and germinomas frequently hyperdense on CT (hypointense T2WI) and prone to CSF dissemination
- Peripheral “exploded” Ca⁺⁺ in PB and central “engulfed” Ca⁺⁺ in germinoma classic but not always identified

PINEOCYTOMAS

Terminology

- Slow-growing pineal parenchymal tumor of young adults composed of small, uniform mature cells resembling pineocytes

Imaging Findings

- Enhancing, circumscribed pineal mass which “explodes” pineal Ca⁺⁺
- May mimic pineal cyst or pineoblastoma

Top Differential Diagnosis

- Pineoblastoma
- Nonneoplastic pineal cyst
- Astrocytoma
- Other germ cell tumors (GCT)

- Meningioma

Pathology

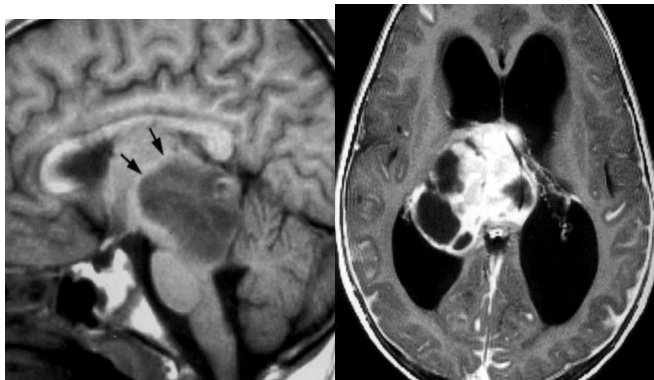
- Pineocytoma and pineoblastomas account for 15% of pineal region neoplasms
- Pineocytomas represents approximately 45% of pineal parenchymal tumors
- Pineal parenchymal tumors << germinoma
- Cysts and small areas of hemorrhage may be seen
- May compress but do not invade adjacent structures
- WHO grade II

Clinical Issues

- Overall 5 year survival 86%

Diagnostic Checklist

- PCs “explode” gland Ca++ while germinomas “engulf” gland Ca++
- Imaging of pineocytoma may be nonspecific



MEDULLOBLASTOMA (PNET-MB)

Terminology

- Medulloblastoma (MB), posterior fossa PNET, PNET-MB
- Malignant, invasive, highly cellular embryonal tumor

Imaging Findings

- Solid mass in 4th ventricle
- Hydrocephalus common (95%)
- > 90% enhance
- Contrast essential to detect CSF dissemination
- Contrast-enhanced MR of spine (entire neuraxis)

Top Differential Findings

- Cerebellar pilocytic astrocytoma (PA)
- Ependymoma
- Choroid plexus papilloma (CPP)
- Atypical teratoid/rhabdoid tumor (AT/RhT)

Pathology

- 15-20% of all pediatric brain tumors
- WHO grade IV

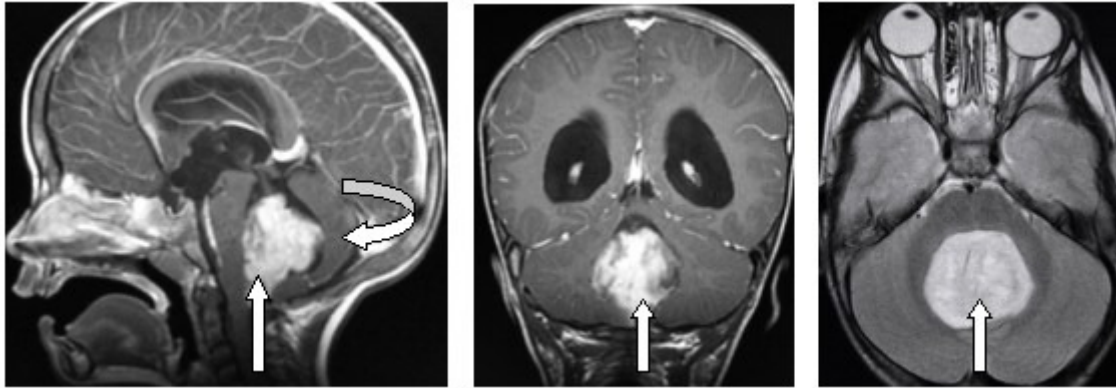
Clinical Issues

- Ataxia, signs of increased intracranial pressure
- Relatively short (< 1 month) of symptoms
- Rapid growth with early subarachnoid spread
- “Standard risk” clinical profile
- “High risk” clinical profile

Diagnostic Checklist

- Remember AT/RhT in patients under 3 years

- 4th V tumor arising from roof = PNET-MB
- 4th V tumor arising from floor = ependymoma



• (Left): MRI Scan (Sagittal View-Gadolinium Enhanced) of a Young child with a large 4th Ventricular Medulloblastoma (Vertical Arrow) with compression of the Cerebellum (Curved Arrow).

Figure 1B (Center): MRI Scan (Coronal View-same patient). The tumor has considerable "enhancement" indicating a substantial blood supply.

Figure 1C (Right): MRI Scan (Transaxial View-same patient). The tumor (Arrow) fills the 4th Ventricle demonstrates extensive "enhancement".

Distinctions among medulloblastoma, ependymoma, and astrocytoma in posterior fossa

<i>Feature</i>	<i>Medulloblastoma</i>	<i>Ependymoma</i>	<i>Astrocytoma</i>

Unenhanced CT	Hyperdense	Isodense	Hypodense
Enhancement	Moderate	Minimal	Nodule enhances, cyst does not
Calcification	Uncommon (10%-21%)	Common (40%-50%)	Uncommon (< 10%)
Origin	Vermis	4 th ventricle ependyma	Hemispheric
T2WI	Intermediate	Intermediate	Bright
Site	Midline	Midline	Eccentric
Subarachnoid seeding	15%-50%	Uncommon	Rare
Age (yr)	5-12	2-10	10-20
Cyst formation	10-20%	15%	60-80%
Foraminal spread	No	Yes (Luschka, Magendie)	No
Hemorrhage	Rare	10%	Rare
MRS			
Metabolite			
NAA	Low	Intermediate	Intermediate
Lactate	Absent	Often present	Often present
Choline	High	Less elevated	High

SUPRATENTORIAL PNET

Terminology

- Supratentorial primitive neuroectodermal tumor (S-PNET)
- Cerebral embryonal tumor composed of undifferentiated neuroepithelial cells

Imaging Findings

- Best diagnostic clue: Large, complex hemispheric mass with minimal peritumoral edema
- Isoattenuating to hyperattenuating
- Calcification (50-70%)
- Hemorrhage and necrosis common
- Heterogeneous enhancement

- DWI: Restricted diffusion common
- Best imaging tool: Enhanced MR of brain and spine
- Adding post-enhanced FLAIR aids in detecting leptomeningeal metastases

Top Differential Diagnosis

- Astrocytoma
- Ependymoma
- Oligodendroglioma
- Atypical teratoid/rhabdoid tumor

Top Differential Diagnosis

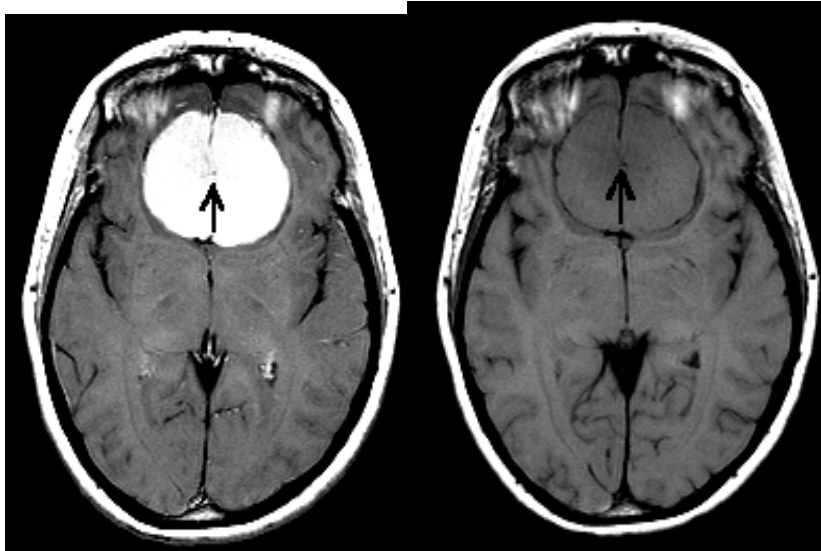
- Astrocytoma
- Ependymoma
- Oligodendroglioma
- Atypical teratoid/rhabdoid tumor

Pathology

- WHO grade IV

Clinical Issues

- Vary with site of origin and size of tumor
- Hemispheric – seizures, disturbed consciousness, motor deficit, elevated ICP
- Suprasellar – visual disturbance, endocrine problems
- Clinical profile: Infant presenting with microcephaly, seizures and large hemispheric mass
- S-PNET → 30-35% 5 year survival



MENINGIOMA

Imaging Findings

- Best diagnostic clue: Dural-based enhancing mass w/cortical buckling & trapped CSF clefts/cortical vessels
- Hyperostosis, irregular cortex, tumoral calcifications, increased vascular markings
- Brain cysts & trapped pools of CSF common
- Peritumoral hypodense vasogenic edema (60%)
- > 95% enhance homogeneously & intensely
- Elevated levels of Alanine at short TE
- DSA: “Mother-in-law” sign → comes early, stays late
- Best imaging tool: MRI + contrast

Top Differential Diagnoses

- Dural metastasis

- Granuloma (sarcoid, TB)
- Idiopathic hypertrophic pachymeningitis
- Extramedullary hematopoiesis

Pathology

- Loss of one copy of chromosome 22 is most prevalent chromosomal change in meningioma
- Arise from arachnoid meningotheial (“cap”) cells
- Most common adult intracranial tumor (13-20%)

Clinical Issues

- < 10% of all meningiomas ever cause symptoms
- Age: Middle decade of life
- Gender: M:F ranges 1: 1.5 to 1:3
- Ethnicity: More common in African-Americans
- Generally grow slowly, compress adjacent structures
- Asymptomatic followed with serial imaging

Diagnostic Checklist

- Preoperatively define ENTIRE tumor extent

Signs of Meningioma

- Iso- or Hypointensity on T2 images
- Inward white matter buckling
- Speckled T2 signal hyperintensity (microcyst formation)
- Focal T2 hypointensity (macrocalcifications)
- Prominent circumferential flow void (hypervascularity)
- Cisternal widening
- Calvarial hypointense T1 and T2 (sclerosis) or hyperintense T2 (edema or hyperemia)
- Pseudocapsule formation due to desmoplasia or fibrosis, displaced dura, CSF, and vessels
- Variable edema (edema can be pronounced)
- En plaque variant, ridge
 - b. Wraps around structures especially basilar skull vessels

- c. Aggressive
- d. Propensity for sphenoidal ridge
- e. Fibrovascular histology more common

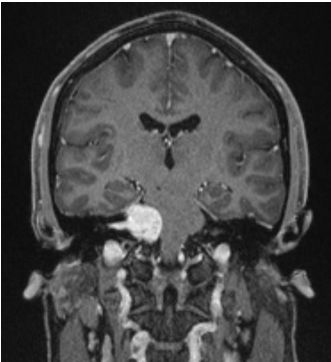
SCHWANNOMA

Terminology

- Benign encapsulated nerve sheath tumor composed of differentiated neoplastic schwann cells

Imaging Findings

- Best diagnostic clue: VS looks like “ice cream on cone”; parenchymal looks like cyst with nodule
- All cranial nerves (exceptions: Olfactory, optic nerves) have myelinated schwann cell sheaths and are sites for intracranial schwannomas
- 1-2% intracerebral



Top Differential Prognosis

- Pleomorphic xanthoastrocytoma (PXA)
- Pilocytic astrocytoma
- Ganglioglioma
- Metastasis
- Hemangioblastoma

Pathology

- Schwannomas = 5-8% of all intracranial neoplasms
- Two types of tissue (Antoni A, B)

Clinical Issues

- Age: 70% of parenchymal schwannomas present before age of 30
- Slowly growing: recurrence after surgery < 10%
- Malignant degeneration exceptionally rare

Diagnostic Checklist

- Cystic, calcified, enhancing hemispheric parenchymal mass in a young patient isn't necessarily a glioma!

Differential diagnosis of meningioma versus schwannoma

<i>Feature</i>	<i>Meningioma</i>	<i>Schwannoma</i>
Dural tail	Frequent	Extremely rare
Bony reaction	Osteolysis or hyperostosis	Rare
Angle made with dura	Obtuse	Acute
Calcification	20%	Extremely rare
Cyst/necrosis	Rare	Up to 10%
Enhancement	Uniform	Inhomogeneous in 32%
Extension into the internal auditory canal	Rare	80%
MRS	Alanine	Taurine, GABA
Precontrast CT attenuation	Hyperdense	Isodense
Hemorrhage	Rare	Somewhat more common

NEUROFIBROMA

Terminology

- Plexiform NF (PNF) = infiltrative extraneural tumor typically associated with neurofibromatosis 1 (NF1)

Imaging Findings

- Best diagnostic clue: “Worm-like” soft tissue mass infiltrative scalp, orbit or parotid in patient with NF1

Top Differential Diagnoses

- Schwannoma
- Malignant peripheral nerve sheath tumor (MPNST)
- Vascular malformation of scalp
- Sarcoma or lymphoma of skull/scalp
- Metastasis
- Chronic interstitial demyelinating polyneuropathy (CIDP)

Diagnostic Checklist

- Look for other stigmata of NF1 (café-au-lait spots, axillary freckling, Lisch nodules, etc)

PEARLS IN THE DIAGNOSIS OF GLOMUS TUMOR

- Age: 30-50 years
- Signal
 - a. Intermediate T1, hyperintense T2
 - b. Punctuate speckled salt and pepper areas pinpoint flow void due to hypervascularity
- Location
 - a. Jugular foramen (50-60%)= glomus jugulare
 - b. Tympanic branch or Jacobson’s nerve, glomus tympanicum (20-30%)
 - c. Auricular branch or Arnold’s nerve, glomus vagale (10%)
 - d. Perianglia cells of the carotid bifurcation= glomus caroticum (less than 10%)Female predilection

- Multiplicity (10%) particularly with multiple endocrine adenomatosis (3%)
- Eight percent harbor other neoplasms
- Most common primary middle ear neoplasm
- Second most common temporal bone neoplasm
- Enhancement: pronounced, early, mottled
- Associated thrombosis or flow phenomenon in the jugular vein
- Shape: Triangular shape in the coronal projection
- Differential diagnosis
 - a. Neuroma: No punctate flow void, more rounded shape
 - b. Meningioma: Flat dural margin, homogeneous enhancement, wraparound vessels with infiltrative growth pattern
 - c. Normal slow flow in jugular vein

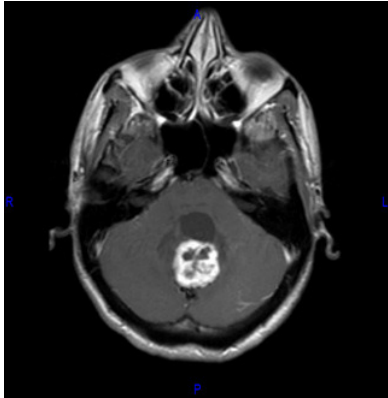
HEMANGIOBLASTOMA

Terminology

- HGBL currently classified as meningeal tumor of uncertain histogenesis (WHO, 2000)

Imaging Findings

- Best diagnostic clue: Adult with intra-axial posterior fossa mass with cyst, enhancing mural nodule abutting pia
- 90-95% posterior fossa
- Size: Size varies from tiny to several cms
- 60% cyst + “mural” nodule
- 40% solid



• **Top Differential Diagnoses**

- von Hippel-Lindau syndrome (VHL)
- Metastasis
- Astrocytoma
- Vascular neurocutaneous syndrome
- Cavernous malformation (CM)
- Clear cell ependymoma

Pathology

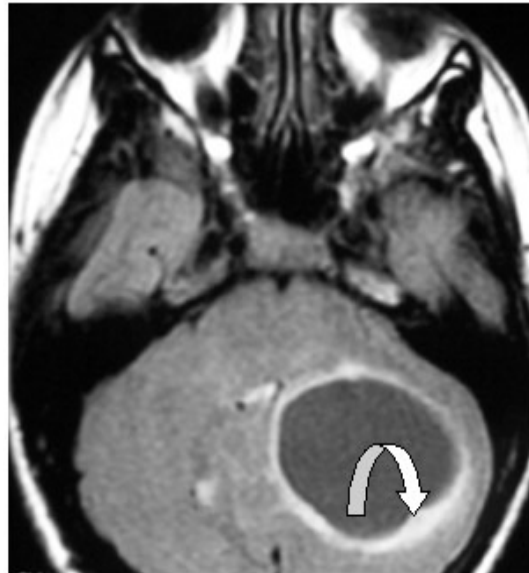
- VHL phenotypes (based on presence, absence of pheochromocytoma and renal cell carcinoma)
- 1-2% of primary intracranial tumors
- 7-100% of posterior fossa tumors
- Secondary polycythemia (may elaborate erythropoietin)
- WHO grade I

Diagnostic Checklist

- Screen entire neuraxis for other HGBLs
- Most common posterior fossa intra-axial mass in middle-aged/older adult = metastasis, not HGBL!

Pearls in the Diagnosis of Hemangioblastoma

- Sixty percent are intramedullary; 40% are extramedullary but intradural
- Thirty percent have Hippel-Lindau disease
- Thoracic location in 50% and cervical location in 40%
- Lesions are single in 80% and multiple in 20%
- Cyst formation in 40%
- MR findings
 - a. Intermediate signal intensity nodule which enhances
 - b. Speckled foci or flow void signal in and about the nodule
 - c. Areas of marginal cyst formation above and below the lesion
 - d. Round or ovoid shape



MRI Scan (Gadolinium Enhanced Axial View) Left Cerebellar Hemisphere Cystic Tumor.

The "Mural Nodule" (Curved Arrow) "enhances" due to its considerable blood supply and is responsible for the formation of the fluid of the cyst. The "Nodule" must be entirely removed in order to "cure" this lesion, particularly in "Sporadically" occurring cases.

Cysts of this size cause considerable pressure on the Brain Stem which can threaten the patient's life if left untreated.

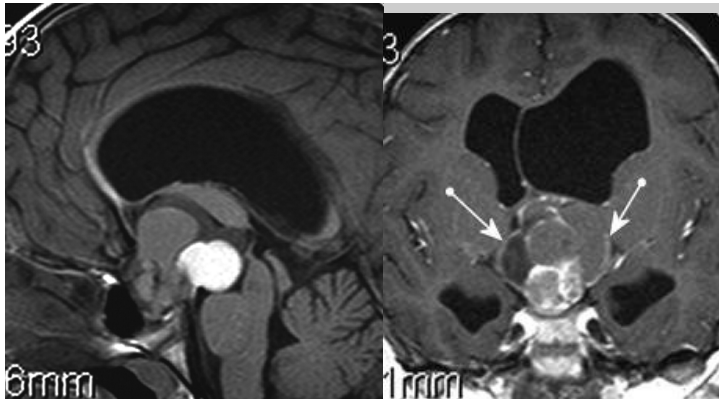
HEMANGIOPERICYTOMA

Terminology

- Sarcoma related to neoplastic transformation of pericytes, contractile cells about capillaries

Imaging Findings

- Lobular enhancing extra-axial mass with dural attachment, +/- skull erosion
- May mimic meningioma, but without Ca++ or hyperostosis
- Typically involve falx, tentorium, or dural sinuses
- Marked enhancement, often heterogeneous



Top Differential Diagnoses

- Meningioma
- Dural metastases
- Lymphoma
- Neurosaroidosis
- Gliosarcoma
- Solitary fibrous tumor

Pathology

- HPC is a distinctive mesenchymal neoplasm unrelated to meningioma
- Represents < 1% of primary CNS tumors
- Represents 2-4% of all meningeal tumors
- WHO grade II or III (anaplastic)

Clinical Issues

- Most common 4th-6th decade, mean age 43 years
- Extracranial metastases common, up to 30%

Diagnostic Checklist

- When a “meningioma” has atypical features (frank bone erosion, multiple flow voids) think HPC!

PEARLS IN THE DIAGNOSIS OF CRANIOPHARYNGIOMA

- Peak age: Biphasic, 3-5 years and 50-60 years
- Location
 - a. Suprasellar (80%)
 - b. Sellar/suprasellar (15%)
 - c. Sellar (4%)
 - d. Third ventricle (0.5%)
 - e. Nasopharynx (0.5%)
- Signal
 - a. Hyperintense T1 & T2: Hydrolyzed cholesterol and/or blood (65%)
 - b. Intermediate T1, hyperintense T2: Keratin (20%)
 - c. Hypointense T2: Calcification (75%)
 - d. Hypointense T1, hyperintense T2: Cyst formation (40%)
 - e. Intermediate T1 and T2: Solid tumor (15%)
- Calcification (75%): Twice as frequent in children as adults (Rathke’s cyst do not calcify)

- Origin: Rathke's cells or pouch having multilayered complex epithelium (Rathke's cysts have a simple single-layered epithelium)
- Enhancement: Variable, none to mild
- Hemorrhage: (10%)
- Differential diagnosis: Meningioma (homogenous, marked enhancement); aneurysm (flow void or clot); pituitary adenoma (more homogeneous signal, noncalcified, usually no hyperintense T1 signal)

PRIMARY CNS LYMPHOMA

Terminology

- Malignant primary CNS neoplasm composed of B lymphocytes

Imaging Findings

- Best diagnostic clue: Enhancing lesion(s) within basal ganglia, periventricular WM
- 90% supratentorial
- Deep gray nuclei commonly affected
- Often involve, cross corpus callosum
- Frequently abut, extend along ependymal surfaces

Top Differential Diagnoses

- Toxoplasmosis
- Glioblastoma multiforme (GBM)
- Abscess
- Progressive multifocal leukoencephalopathy (PML)

Pathology

- 98% B cell, non-Hodgkin lymphoma (NHL)
- Incidence increasing in immunocompetent, immunocompromised
- 1-7% of primary brain tumors, incidence rising
- Represents approximately 1% of lymphomas

Clinical Issues

- Median survival 17-45 months

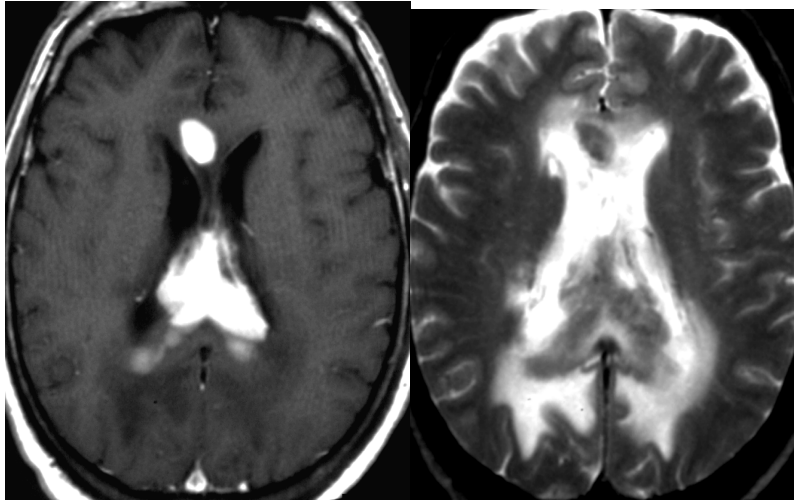
- AIDS median survival 2-6 months
- Stereotactic biopsy, followed by radiation therapy and chemotherapy

Diagnostic Checklist

- Imaging and prognosis varies with immune status
- Periventricular location and Subependymal involvement is characteristic of PCNSL
-

PEARLS IN THE DIAGNOSIS OF PRIMARY & SECONDARY BRAIN LYMPHOMA

- Location
 - a. Deep white gray matter (70%)
 - b. Leptomeningeal signal: Intermediate T1 and isointense to hyperintense T2 (30%)
- Enhancement: Marked
- Margin: Sharply marginated intra-axial lesions which may be large, and round or oval in shape
- Edema: Mild to moderate
- Cyst formation: Extremely rare
- Hemorrhage
- Calcification: Rare
- Multiplicity: Extremely common
- Tipoff: Clinical history of immunosuppression or AIDS



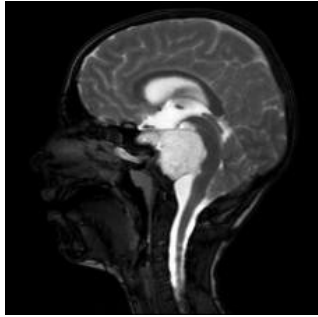
CHORDOMA

Terminology

- Malignant tumor arising from notochord remnants

Imaging Findings

- Mass is hyperintense to discs on T2WI, with multiple septa
- Histologic identification of physaliphorous cell confirms diagnosis
- Location: Sacrococcygeal > spheno-occipital >> vertebral body
- Size: Several cm at presentation
- Morphology: Midline lobular soft tissue mass with osseous destruction
- May extend into disc, involve 2 or more adjacent vertebrae
- May extend into epidural/perivertebral space, compress cord
- May extend along nerve roots, enlarge neural foramina
- Amorphous intratumoral Ca⁺⁺



Pathology

- 3 types described
- Typical: Lobules, sheets, and cords of clear cells with intracytoplasmic vacuoles (physaliphorous cells); abundant mucin
- Chondroid: Hyaline cartilage (usually sphenoid-occipital region)
- Dedifferentiated: Sarcomatous elements (rare, highly malignant)

Pearls in the Diagnosis of Chordoma

- Age: 30-40 years
- Location:
 - Sacrum 50%
 - Clivus 30%
 - Cervical (C2) 20%
- Intermediate T1 signal, mottled hyperintense T2 signal
- Calcification 30-50%
- Enhancement: none to mild
- Shape: cauliflower-like shape in the C2 and clival regions
- Tipoffs: cauliflower-shaped or exophytic mass involving intervertebral disc (sacrum) or straddling the clivus or C2 anteriorly and posteriorly in the sagittal projection

PARENCHYMAL METASTASES

Terminology

- Parenchymal tumors that originate from, but are discontinuous with, other CNS primary or extracranial systemic neoplasms

Imaging Findings

- Best diagnostic clue: Discrete parenchymal mass(es) at gray-white interface
- Best imaging tool: Contrast-enhanced MRI >> CECT
- Protocol advice: Double or triple-contrast dose increases sensitivity but questionable value on routine basis

Top Differential Diagnoses

- Abscess
- Malignant glioma
- Thromboembolic stroke(s)
- Demyelinating disease

Pathology

- Prevalence of metastases vs primary CNS neoplasms increasing
- Now account for up to 50% of all brain tumors
- Seen in 25% of cancer patients at autopsy
- Metastases usually displace rather than infiltrate tissue

Clinical Issues

- Median survival with whole brain XRT = 3-6 months

Diagnostic Checklist

- White matter disease (“UBOs”) in elderly patient can be caused by multifocal metastases
- Use contrast-enhanced scans

PEARLS IN THE DIAGNOSIS OF METASTATIC DISEASE

Hemorrhagic Metastases

- Choriocarcinoma: 90-95%
- Melanoma: 85%

- Hypernephroma: 65%
- Thyroid carcinoma: 55%
- Lung carcinoma: 15%
- Breast carcinoma: 10%
- Alimentary tract carcinoma: 5-10%
- Other: Less than 5%

Subtypes with a Lower Propensity toward Brain Metastases

- Squamous cell carcinoma
- Sarcoma

Primary Brain Tumors Which May Metastasize Peripherally

- Medulloblastoma
- Cerebellar sarcoma
- Glioblastoma multiforme

Subependymal or Intraventricular Tumor Spread

- Melanoma
- Lymphoma
- Breast carcinoma
- Lung carcinoma

Leptomeningeal or Dural Carcinomatosis

- Breast carcinoma
- Lung carcinoma (adenocarcinoma)
- Melanoma
- Lymphoma

Brain Metastases without Edema

- Squamous cell carcinoma

Cystic Metastases

- Lung carcinoma (oat cell)
- Radiated metastases

Isointense Metastases

- Metastatic colon carcinoma (70%)
- Prostate carcinoma (60%)
- Osteogenic sarcoma
- Melanoma (30%)

Pure Cortical Metastases

- Melanoma
- Choriocarcinoma
- Lung carcinoma

Intraventricular Choroidal Metastases

- Lung carcinoma
- Colon carcinoma
- Breast carcinoma

INTRACRANIAL CYSTS ON MR

- Arachnoid cyst: Extra-axial, no edema, non-enhancing
- Cystic neoplasm (low tumor density): Edema, enhances
- Chronic subdural hematoma or hygroma: Extra-axial
- Suprasellar cyst from dilated third ventricle
- Interhemispheric cyst from porencephaly
- Posterior fossa cyst form of Dandy-Walker malformation
- Enlarged cisterna magna
- Post-infarct cystic encephalomalacia

- Cysts associated with isodense tumors
 - a. Ganglioma: May calcify
 - b. Cerebellar hemangioblastoma
 - c. Cystic astrocytoma: Enhancing nodule
- Cysticerosis: Calcification

ARACHNOID CYST

Terminology

- Arachnoid cyst (AC), subarachnoid cyst
- Intra-arachnoid CSF-filled sac that does not communicate with ventricular system

Imaging Findings

- Best diagnostic rule: Sharply demarcated round/ovoid extra-axial cyst that follows CSF attenuation/signal
- 50-60% middle cranial fossa (MCF)
- Sharply-marginated extra-axial fluid collection isointense with CSF
- FLAIR: Suppresses completely with FLAIR
- DWI: No restriction

Top Differential Diagnoses

- Epidermoid cyst
- Chronic subdural hematoma
- Subdural hygroma
- Other nonneoplastic cysts

Pathology

- 1% of all intracranial masses
- If in middle fossa, temporal lobe may appear (or be) hypoplastic
- Subdural hematoma (increased prevalence, especially MCF)
- Acs displace but don't engulf vessels, cranial nerves

Clinical Issues

- Often asymptomatic, found incidentally

Diagnostic Checklist

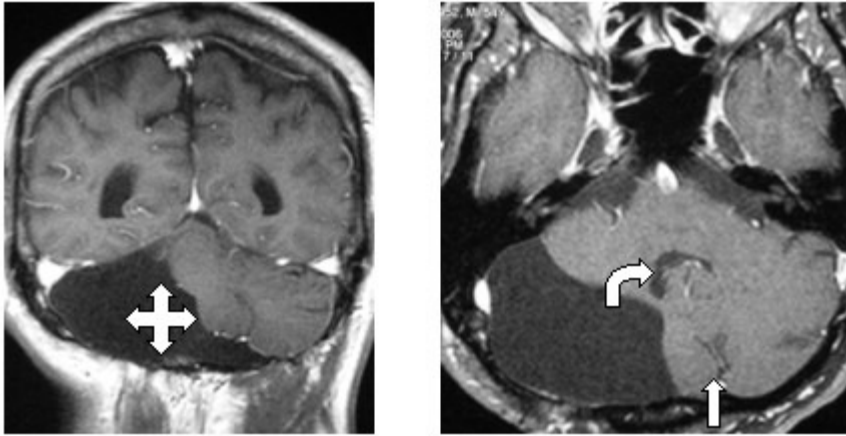
FLAIR, DWI best sequences for distinguishing etiology of cystic-appearing intracranial Pearls in the Diagnosis of Arachnoid Cyst

- Location: extra-axial
 - a. Middle cranial fossa, peritemporal
 - b. Cerebral convexity
 - c. Posterior fossa, retrocerebellar
 - d. Suprasellar quadrigeminal plate cistern
- Homogeneous water-like signal, hypointense on T1 and very hyperintense on T2 (Remember that pulsation in the cyst may create the false impression of a nodule inside)
- There should be no evidence of intra-axial edema
- The margins of the lesion are smooth, sharp and straight, particularly in the middle fossa cysts along the posterior margin
- Suprasellar cysts are oval or square in shape, splay the cerebral peduncles and carotid termini, and push the mamillary body upward and posterior

Differential Diagnosis

- Epidermoid: Hypointense T1, mixed hyperintense T2, does not match CSF fluid
- Ependymal- or nonependymal-lined cyst: Intra-axial
- Craniopharyngioma: Mixed T1 and T2 signal, variable hyperintense fat
- Dermoid tumor: Hyperintense T1 & T2
- Cystic glioma: Hypointense T1, hyperintense T2, intra-axial with surrounding edema

- Masses



This is a series of MRI Scans of a 54 year old Male who complained about recent hearing impairment and ringing ("Tinnitus") in his Right ear. The scans show a large Arachnoid Cyst in the Right Cerebellar Pontine Angle of the Posterior Cranial Fossa.

DERMOID CYST

Imaging Findings

- Best diagnostic clue: Fat appearance + droplets in cisterns, sulci, ventricles if ruptured
- T1 C+: With rupture: Extensive MR enhancement possible from chemical meningitis
- Use fat-suppression sequence to confirm diagnosis

Top Differential Diagnoses

- Epidermoid cyst
- Craniopharyngioma
- Teratoma

Pathology

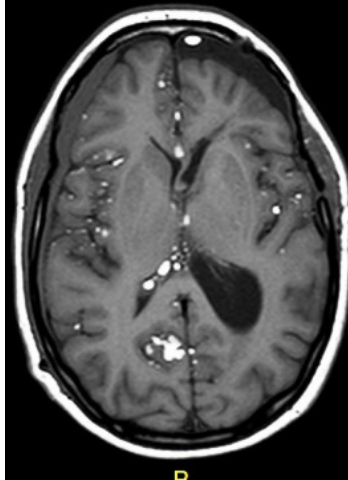
- Rare: < 0.5% of primary intracranial tumors
- Unilocular cyst with thick wall of connective tissue

Clinical Issues

- Uncomplicated dermoid: Headache (32%), seizure (30%) are most common symptoms
- 30-50 y
- Gender: Slight male predilection
- Larger lesions associated with higher rupture rate
- Rupture can cause significant morbidity/mortality
- Rare malignant transformation into SCCa
- Treatment: Complete microsurgical excision

Diagnostic Checklist

- Follows fat characteristics on NECT and T1WI fat-suppressed MRI



EPIDERMOID CYST

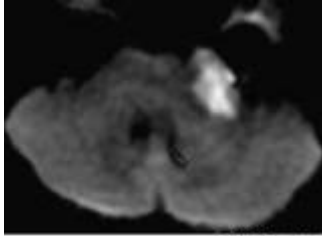
Terminology

- Intracranial epidermoids are congenital inclusion cysts

Imaging Findings

- Best diagnostic clue: CSF-like mass insinuates cisterns, encases nerves/vessels

- Morphology: Lobulated, irregular, “cauliflower-like” mass with “fronds”
- FLAIR: Usually doesn’t completely null
- Restricted diffusion yields high signal



Top Differential Diagnoses

- Arachnoid cyst
- Inflammatory cyst (i.e., neurocysticercosis)
- Cystic neoplasm
- Dermoid cyst

Pathology

- 0.2-1.8% of all primary intracranial tumors

Clinical Issues

- Most common symptom: Headache
- Cranial nerve 5,7,8 neuropathy common
- Age: Presents at 20-60 y with peak at 40
- Grows slowly: Epithelial component growth rate commensurate to that of normal epithelium
- Rare malignant degeneration into squamous cell carcinoma (SCCa) reported
- Treatment: Microsurgical resection

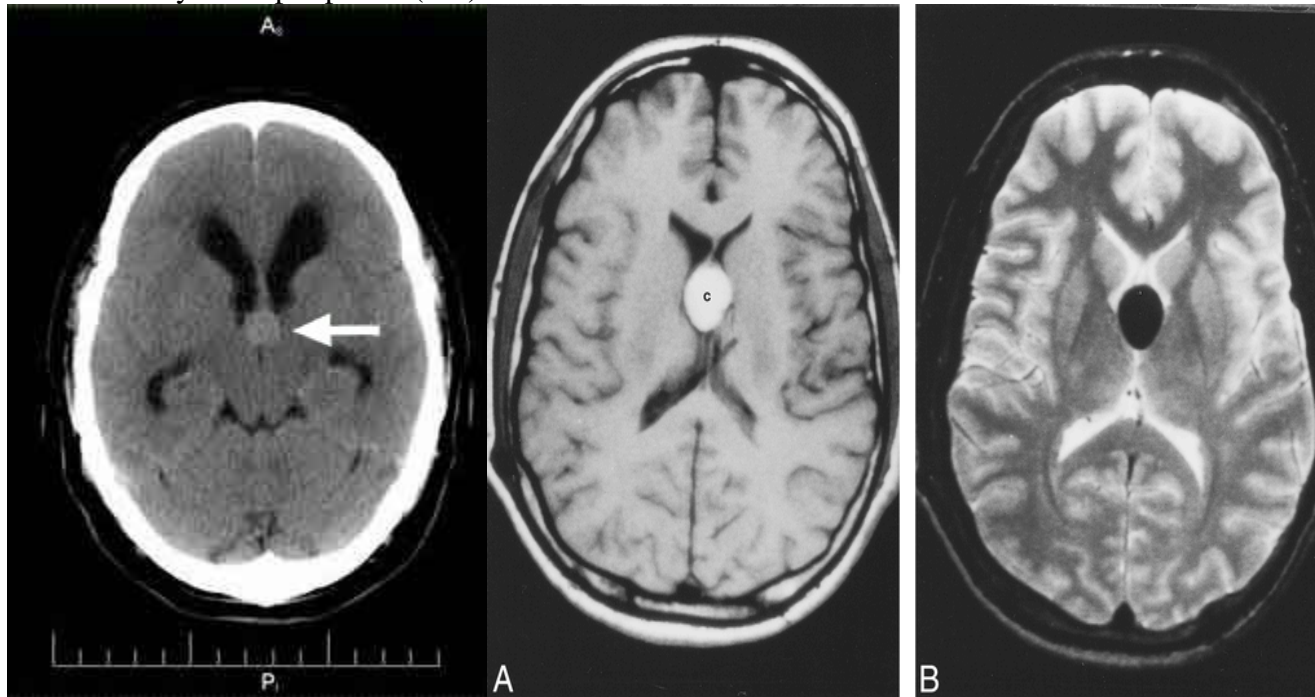
Diagnostic Checklist

- Resembles CSF on imaging studies, except usually incomplete nulling on FLAIR
-

COLLOID CYST

Imaging Findings

- Best diagnostic clue: Hyperdense foramen of Monro mass on NECT
- Most anterosuperior ventricle location
- Size < 1.5 centimeters
- No or nominal contrast enhancement
- Density correlates inversely with hydration state
- 2/3 hyperintense on T1WI
- Majority isointense to brain on T2WI (small cysts may be difficult to see!)
- 25% mixed hypo/hyper (“black hole” effect)
- Rare: May show peripheral (rim) enhancement



Indirect Signs

- Intermittent hydrocephalus
- Paramagnetic

Appearance of Colloid Cysts by Signal Intensity

- Paramagnetic type, most common (60%): Hyperintense T1, hypointense T2, peripheral hyperintense T2 rim*
- Cystic type, uncommon (20%): Hypointense T1, hyperintense T2
- Isointense type, rare (10%): Isointense T1 and isointense or minimally hyperintense T2
- Mixed type, rare (less than 10%): Hyperintense T1, isointense T2

*Fluid levels with T2 hypointensity layering dependently are seen in 30-40% of cases.

Top Differential Diagnoses

- Neurocysticercosis
- CSF flow artifact (MR “pseudocyst”)
- Neoplasm
- Choroid plexus mass

Pathology

- From embryonic endoderm, not neuroectoderm!
- 0.5 – 1.0% primary brain tumors
- 15-20% intraventricular masses

Clinical Issues

- Headache (50-60%)
- 3rd-4th decade
- 90% stable or stop enlarging
- 10 % enlarge
- May enlarge rapidly, cause coma/death!

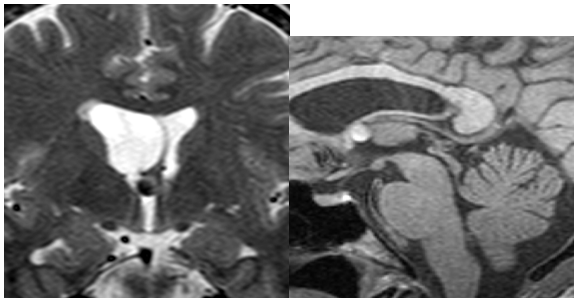
Diagnostic Checklist

- Notify referring MD immediately if CC identified (especially if hydrocephalus is present)

Pearls in the Diagnosis of Colloid Cysts

- Signal intensity similar to hemorrhagic cysts or cystic craniopharyngioma
- Paramagnetic type, most frequent

- Most anterosuperior third ventricle location
- Intermittent hydrocephalus
- Minimal enhancement on CEMR
- Internal constituents include calcium, magnesium, copper, iron, manganese, and sodium
- Rare in the pediatric population
- May simulate melanoma metastases



RADIATION NECROSIS & RECURRENT NEOPLASM

Radiation Necrosis

- Hypointense T1, iso- to hyperintense T2, variable central Hypointensity Enhancement is corrugated, wavy & irregular (wrinkled configuration)

Recurrent Neoplasm

- Variable T1 and T2
- Masslike & Nodular
- Edema has no respect for the forceps major or corpus callosum
- Metabolism on Pet usually equals or exceeds that of white matter
- May recur early or late

SIGNS OF INTRACRANIAL NEOPLASTIC HEMORRHAGE

- Intermediate signal intensity on T1 and T2
- Signal alteration which does not correspond to any known pattern of blood evolution over an appropriate period of time
- Delayed temporal resolution of hemorrhage
- Bizarre or complex signal intensities
- Irregular, absent or complex hemosiderin rings
- Persistent or exaggerated edema
- Lesion multiplicity
- Absence of hypointense calcification
- Disproportionate mass effect for lesion size
- Nodular enhancement

FREQUENCY OF HEMORRHAGE IN INTRACRANIAL NEOPLASMS

- Pineal choriocarcinoma or teratocarcinoma (90%)
- Primary intracranial neuroblastoma (85%)
- Oligodendroglioma (80%)

- Melanoma (70%)
- Ependymoma (55%)
- Glioblastoma multiforme or high-grade astrocytic neoplasm (35%)
- Metastasis (especially renal cell, thyroid, bronchogenic, melanoma and choriocarcinoma)
- The frequency of intracranial neoplastic hemorrhage increases dramatically after cranial irradiation

CYSTIC PITUITARY MASSES

Empty Sella

- Homogeneous T1 hypointensity, T2 hyperintensity: Pure water signal
- Midline pituitary stalk
- Paucity of solid pituitary tissue
- No evidence of chiasmatic or suprasellar mass effect
- Enhancement of normal pituitary tissue only

Arachnoid Cyst

- Homogenous T1 hypointensity, T2 hyperintensity: Pure water signal
- Sellar, suprasellar, retrosellar, and perisellar mass effect are common
- Effaced and displaced pituitary stalk, multidirectional
- Enhancement of normal pituitary tissue

Cystic Craniopharyngioma

- May have foci of T1 hyperintensity
- May have hypointense T2 calcification
- Suprasellar +/- intrasellar extension
- Mixed enhancement

Cystic Pituitary Adenoma or Neuroectodermal Tumor

- Moderate T1 hypointensity, T2 hyperintensity: Proteinaceous water signal (therefore no exact CSF match)
- Displaced pituitary stalk
- Hormonal abnormalities frequently present
- Intra- and suprasellar mass effect and/or extension

- Foci of nodular enhancement from solid components

Dermoid

- Hyperintense T1, hyperintense T2
- Predominantly suprasellar
- Nonenhancing

Epidermoid

- Hypointense T1, hyperintense T2
- Inhomogeneous
- Minimal peripheral enhancement
- Irregular shape

Cystic Optic Chiasmatic/Hypothalamic Glioma

- Neurofibromatosis frequently associated
- Origin in, or involvement of, the optic chiasm or hypothalamus
- Mild enhancement

CRITERIA FOR SELLAR MICROADENOMA

Direct Criteria

- T1 hypointensity < 1 cm in size
- Hypointense on CEMR < 8 minutes, can be isointense 8-40 minutes and hyperintense on CEMR > 40 minutes

Indirect Criteria

- Stalk deviation
- Abnormal gland height (greater than)
 - a. 6-7 mm male or prepubescent
 - b. 7-11 mm gravid female postpuberty
 - c. 10-13 mm female, peripartum
- Floor deviation
- Gland size asymmetry

PEARLS IN THE DIAGNOSIS OF PITUITARY MACROADENOMA

- Greater than 1 cm
- Isointense on T1
- Iso- or hyperintense on T2 with mild to moderate enhancement
- Diaphragma sellar notching helps differentiate extrasellar mass growing down from pituitary mass growing up
- Complications of macroadenoma
 - a. Chiasmatic compression
 - b. Cavernous sinus invasion
 - c. Prolactin levels > 2,000 picograms/dl implies cavernous invasion
- Cont. of Complications of macroadenoma
 - ii. Abuts the lateral dural sinus walls
 - iii. Loss of speckled signal in the cavernous sinus distribution
 - c. Pituitary hemorrhage or apoplexy
 - d. Pituitary adenoma recurrence
 - e. Differential diagnosis of macroadenoma
 - i. Craniopharyngioma
 - ii. Meningioma (dark-isointense)
 - iii. Aneurysm (lamellated)
 - iv. Metastases (isointense-bright)

INTRASELLAR PITUITARY SIGNAL VOIC OR HYPOINTENSITY

Common

- Volume averaging of the parasellar carotid artery dura and CSF

Uncommon

- Aneurysm of the paracavernous carotid artery

Rare

- Vascular malformation of the paracavernous carotid artery
- Primitive trigeminal artery aneurysm
- Pituitary
- Intracavernous calcified meningioma
- Pituitary gas associated with abscess formation or prior surgery
- Intracavernous calcified craniopharyngioma
- Postsurgical intracavernous susceptibility effect (clip, metal, etc.)

INTRACRANIAL SIGNAL: HYPERINTENSE T1, HYPOINTENSE T2

Common

- Subacute hematoma or clot (mid or high field)
- Flow (first echo slice entry phenomenon)
- Melanoma metastases
- Hemorrhagic metastases (choriocarcinoma, neuroblastoma, embryonal cell carcinoma, thyroid carcinoma, renal cell carcinoma, malignant melanoma)
- Lipoma
- Pantopaque

Uncommon Colloid cyst

- Calcified xanthogranuloma
- Aneurysm (with clot or slice entry)

- Craniopharyngioma

INTRACRANIAL SIGNAL: HYPO-TO ISOINTENSE T1, HYPOINTENSE T2 (1.5T)

Common

- Acute hematoma
- Flow (first echo flow void, second echo rephasing)
- Aneurysm with flow phenomenon or acute clot
- Calcification (nontraumatic, nonhemorrhagic)
- Brain iron
- Neoplasm with acute hemorrhage or extensive calcification
- Meningioma
- Metastases (colon, prostate, osteogenic sarcoma, breast)



Uncommon

- Colloid cyst
- Melanoma

Rare

- Choroma

INTRACRANIAL SIGNAL: ISOINTENSE-T1 & T2

Common

- Hyperacute hematoma (transition to acute hematoma [1.5 T])
- Acute hematoma (mid field [0.5 T])
- Subacute hematoma (high field)

- Flow (combinations of flow void adding to flow-related hyperintensity)
- Aneurysm with flow phenomenon
- Meningioma
- Brain iron (low field)
- Isointense metastases (colon, prostate, osteogenic, sarcoma, breast)
- Hamartoma

Uncommon

- Colloid cyst

Rare

- Medulloblastoma or adult cerebellar sarcoma
- Lymphoma
- Tuberculoma
- Chloroma

BLACK SIGNAL

- Flow
- Air or gas
- Hemosiderin (T2 dependent)
- Iron, copper or metal
- Bone
- Calcium
- Superparamagnetic contrast agents
- Ligaments, tendons, fascia
- Magnetic susceptibility
-

HYPPOINTENSE RINGS

- Hemosiderin ring: Chronic hematoma
- Susceptibility rim artifact: Glial or astrocytic neoplasm
- Pseudocapsule of dura, cerebrospinal fluid, cleft, desmoplasia, vessels: Meningioma
- Fibrous rim: Abscess, neurocysticercosis, meningioma

INTRAVENTRICULAR MASSES

Hypointense T1, Hyperintense T2, Nonenhancing

- Arachnoid cyst
- Cysticercosis
- Colloid cyst (3rd ventricle)
- Cystic craniopharyngioma
- Cystic meningioma
- Dandy-Walker cyst (4th ventricle)
- Epidermoid (4th ventricle)
- Neuroepithelial cyst, intraventricular type
- Neuroepithelial cyst (xanthogranuloma of the choroid plexus)

CSF Signal Mass

- Arachnoid cyst
- Cysticercosis
- Dandy-Walker cyst or variant (4th ventricle)
- Mega cisterna magna (pseudocyst)
- Trapped ventricle (pseudomass) Hypointense T1 & T2, Enhancing
- Acute hematoma
- Calcified giant cell astrocytoma
- Calcified flomus of choroid plexus

- Dense or calcified metastases (prostate, colon, osteogenic sarcoma)
- Heavily calcified meningioma
- Hemorrhagic ventricular metastases

Hyperintense T1, Hypointense T2

- Colloid cyst
- CSF flow
- Dermoid
- Early subacute hemorrhage
- Intraventricular craniopharyngioma (heavily calcified)
- Lipoma
- Pantopaque
- Xanthogranuloma of the choroid plexus

Hyperintense T1 & T2

- Dermoid
- Flow
- Intraventricular craniopharyngioma (3rd ventricle)
- Late subacute hemorrhage

Intraventricular Masses by Site

	<i>Lateral</i>	<i>Third</i>	<i>Fourth</i>
NEOPLASMS			
Choroid plexus papilloma/ca	Common, pediatric	Common from	Common, adult

Craniopharngioma Ependymoma Medulloblastoma		suprasellar growth	
Meningioma	Common, glomus, atrium		Along choroid plexus
Metastases	Yes	Yes	Yes
Choroid	Rare	Typical	Not reported

Differential of temporal lobe lesions

<i>Tumor</i>	<i>Age</i>	<i>Demarcation</i>	<i>Edema?</i>	<i>Percent of Tumors Causing Temporal Lobe Seizures</i>	<i>Hemorrhage</i>	<i>Cyst Formation</i>	<i>Enhancement</i>	<i>Cortical Involvement</i>	<i>Calcification</i>
Ganglioglioma	0-30	Well	Very little	40%	Rare	Common	Uncommon	Common	Variable
Low grade astrocytoma	0-30	Well	Yes	26%	Rare	Common	Uncommon	Uncommon	Variable to uncommon
DNET	10-20	Well	None	18%	Common	Common, dominant multiple	Uncommon to variable	Always	Common
Oligodendroglioma	30-60	Less well	Yes	6%	Variable	Variable	Common	Variable	Common
PXA	10-35	Well, but malignant change in 20%	Uncommon	4%	Rare	Common	Common in mural nodule	Common, meningeal attachment	Rare
Desmoplastic infantile ganglioglioma	0-1	Well	Occasionally	< 3%	No	Common	Common in nodule demoplasia	Dural attachment	None

Scar versus residual tumor

<i>Feature</i>	<i>Scar</i>	<i>Tumor</i>
Enhancement within 1-2 days	No	Yes
Enhancement after 3-4 days	Yes	Yes
Change in size with time	Decreases	Increases
Type of enhancement	Linear, outside preoperative tumor bed	Nodular, solid
Mass effect edema	Decreases	Increases

